Series study of percolation moments in general dimension

Joan Adler
School of Physics and Astronomy, Beverly and Raymond Sackler Faculty of Exact Sciences, Tel Aviv University, 69978 Tel Aviv, Israel
and Department of Physics, Technion-IIT, 32000 Haifa, Israel

Yigal Meir and Amnon Aharony
School of Physics and Astronomy, Beverly and Raymond Sackler Faculty of Exact Sciences, Tel Aviv University, 69978 Tel Aviv, Israel

A. B. Harris
School of Physics and Astronomy, Beverly and Raymond Sackler Faculty of Exact Sciences, Tel Aviv University, 69978 Tel Aviv, Israel
and Department of Physics, University of Pennsylvania, Philadelphia, Pennsylvania 19104
(Received 16 January 1989)

Series expansions for general moments of the bond-percolation cluster-size distribution on hypercubic lattices to 15th order in the concentration have been obtained. This is one more than the previously published series for the mean cluster size in three dimensions and four terms more for higher moments and higher dimensions. Critical exponents, amplitude ratios, and thresholds have been calculated from these and other series by a variety of independent analysis techniques. A comprehensive summary of extant estimates for exponents, some universal amplitude ratios, and thresholds for percolation in all dimensions is given, and our results are shown to be in excellent agreement with the ϵ expansion and some of the most accurate simulation estimates. We obtain threshold values of 0.2488 ± 0.0002 and $0.180\,25\pm0.000\,15$ for the three-dimensional bond problem on the simple-cubic and body-centered-cubic lattices, respectively, and $0.160\,05\pm0.000\,15$ and $0.118\,19\pm0.000\,04$, for the hypercubic bond problem in four and five dimensions, respectively. Our direct exponent estimates are $\gamma=1.805\pm0.02$, 1.435 ± 0.015, and 1.185 ± 0.005, and $\beta=0.405\pm0.025$, 0.639 ± 0.020, and 0.835 ± 0.005 in three, four, and five dimensions, respectively.

I. INTRODUCTION

Percolation models have been used to describe geometric phase transitions in a large variety of systems.[1,2] In these systems objects such as sites, bonds, and plaquettes (disks, etc.) on some underlying lattice (continuum) are occupied with probability p. If a sufficient number of these are occupied then there will be an (infinite) connected cluster spanning the system. In the presence of a connected cluster passage of fluid, magnetic order or electric current can be made across the system. The transition from the disordered or insulating phase to the magnetic or conducting one occurs at some threshold concentration, p_c. The transitions are characterized by a singularity in the order parameter, i.e., in the percolation probability (the probability that if a bond is occupied it belongs to the infinite cluster), $P(p)$, which behaves as ($d\neq6$)

$$P(p)=A_p(p-p_c)^{\beta}[1+a_p(p-p_c)^{\Delta_1}+\ldots], \quad (1.1)$$

and by a divergence in the percolation susceptibility, i.e., in the mean finite cluster size, $S(p)$. The divergence of $S(p)$, when p approaches p_c from below, is believed to take the form

$$S(p)=A_2(p_c-p)^{-\gamma}[1+a_2(p_c-p)^{\Delta_1}+\ldots] \quad (1.2)$$

for $d\neq6$, and

$$S(p)=A_2(p_c-p)^{-\gamma}|\log(p_c-p)|^{\theta} \quad (1.3)$$

for $d=6$, with $\gamma=1$ and $\theta=\frac{2}{7}$.[3] The exponent values and certain ratios of critical amplitudes (such as A_p and A_2), are believed to be universal for a given spatial dimension,[4] whereas the threshold estimates are known to be non universal, i.e., lattice and object dependent. For $d>6$, $\gamma=\beta=1$.

In this paper we review previous results for percolation critical data and present new low-density 15-term series in general dimension for bond percolation on hypercubic lattices. This is one term more than previously published for three dimensions and four terms more for higher dimensions. We calculate the jth moments of the percolation cluster-size distribution, which are believed to behave as

$$\Gamma_j(p)=A_j(p_c-p)^{-\gamma_j}[1+a_j(p_c-p)^{\Delta_1}+\ldots], \quad (1.4)$$

where $\gamma_j=\gamma+(j-2)\Delta$ and $S(p)=\Gamma_2$. The gap exponent, Δ, is equal to $\gamma+\beta=D\nu$, where D is the fractal dimensionality of clusters on a length scale that is large

compared to the lattice constant but small compared to the correlation length $\xi \sim (p - p_c)^{-\nu}$. Moment series to 11th order have previously been calculated[5] and a full discussion of the scaling of these moments has been presented in Ref. 5. We assumed there that all the moments in a given dimension will have the same Δ_1, although the a_j could be very different.

A very large number of numerical and analytic calculations have been made for different percolation systems in two[6-15] and three[16-30] dimensions; rather less attention[5,14,27-28,30-34] has been paid to higher-dimensional systems. We give a comprehensive summary of extant results for different dimensions in Tables I (critical exponents) and II (thresholds for hypercubic bond percolation). We have not given all the older results and refer the interested reader to Ref. 12 (two dimensions), Ref. 21 (three dimensions), and Ref. 33 ($d \geq 4$).

For two dimensions the exact values of the exponents proposed[6] for the $q \to 1$ Potts model together with the exact p_c estimates[7,8] have meant that the transition is extremely well characterized. Some previous doubts concerning the reliability of various assumptions and calculations in two dimensions have now been laid to rest. In particular, doubts[9] concerning the exponent estimates ob-

TABLE I. Percolation critical exponents.

Method	β	γ	ν	Δ	Δ_1	$\eta=(2-\gamma/\nu)$
			$D=2$			
Exact[a]	$0.138\dot{8}$	$2.388\dot{8}$	$1.333\dot{3}$	$2.527\dot{7}$		$0.208\dot{3}$
			$D=3$			
Series[b]	0.463					
Series[c]	0.454±0.008	1.73±0.03	0.88±0.02	2.18±0.04		0.03±0.03
Bond[c]	0.474±0.014					
Site[c]	0.40±0.035					
Series[d]	0.435±0.035				1.05±0.15	−0.01±0.09
Series[e]	0.44±0.1	1.79		2.23±0.05		
Monte Carlo[f]			0.89±0.01			−0.04±0.04
Monte Carlo[g]	0.43±0.04		0.88±0.05		0.65±0.1	−0.02±0.04
T matrix[h]		1.71±0.06	0.90±0.02			
Scaling field[i]			0.71		0.81	0.17
ϵ expansion[j]	0.34±0.04	1.82±0.04	0.83±0.01	2.16±0.04	1.59−1.94[o]	−0.18±0.02
Three-loop vertex[k]	0.34	1.75	0.81	2.09		−0.16
Five-loop vertex[k]		1.74±0.015				−0.131±0.001
Monte Carlo[q]	0.412±0.010	1.795±0.005	0.875±0.008	2.207±0.005		−0.05±0.025
This work	0.405±0.025	1.805±0.02	0.872±0.070	2.21±0.04	1.1±0.2	−0.07±0.05
			$D=4$			
Series[e]	0.665±0.15	1.44±0.05		2.10±0.04		
Series[l]	0.64					
MCRG[m]	0.56		0.64			
Monte Carlo[g]	0.65±0.04		0.68±0.03		0.65±0.2	−0.10±0.09
Monte Carlo[n]	0.5	1.6±0.1				
Scaling field[i]			0.58		0.78	0.034
ϵ expansion[j]	0.64±0.02	1.44	0.68	2.08±0.02	0.88−1.0[o]	−0.12±0.04
This work	0.639±0.020	1.435±0.015	0.678±0.050	2.074±0.006	0.65±0.10	−0.12±0.04
			$D=5$			
Series[e]	0.83±0.1	1.20±0.03		2.025±0.055		
Series[l]	0.84					
MCRG[m]	0.67		0.51			
Monte Carlo[n]	0.7	1.3±0.1				
Scaling field[i]			0.53		0.65	−0.005
ϵ expansion[j]	0.835±0.005	1.18	0.57	2.02±0.005	0.42−0.45[o]	−0.070
This work	0.835±0.005	1.185±0.005	0.571±0.003	2.02±0.01	0.55±0.15	−0.075±0.020

[a]Reference 6.
[b]Reference 20; the error is $\pm 0.013\,12\Delta p_c$.
[c]Reference 21.
[d]Reference 22.
[e]References 5 and 33.
[f]Reference 18.
[g]Reference 26.
[h]Reference 29.
[i]Reference 19.
[j]Reference 30 (third order).
[k]Reference 16.
[l]Reference 34.
[m]Reference 32.
[n]Reference 31.
[o]Private communication from J. Green, third order.
[p]Reference 37.

tained from series were resolved[11,12] by using nonanalytic confluent corrections to scaling [i.e., $\Delta_1 \neq 1.0$ in Eq. (1.1)]. Also, all the current series values in two dimensions are in excellent agreement (both for exponents and for amplitude ratios[5,13]) with their ϵ-expansion counterparts, even at $d=2$, so there exists no evidence for a new fixed point appearing somewhere below three dimensions.[10] The series results are also in agreement with hyperscaling.[15]

Despite the exact exponent and threshold values and the resolution of the various discrepancies there is still a problem with two-dimensional (2D) percolation. Recently, questions have been raised concerning the universality of certain amplitude ratios between lattice and continuum percolation.[17] If these ratios are indeed different then there must be a basic questioning of our ideas concerning universality, since the measured critical exponents for lattice and continuum percolation appear to agree. If the ratios can be shown to agree with each other then we must question the simulations (or rather the extrapolations and error bounds on the result from the simulations) that led to the differences. As a step towards the resolution of this controversy, careful new estimates of all critical amplitude ratios for 2D percolation are highly desirable. We have evaluated several such ratios in general dimension.

For three dimensions the critical behavior is less well documented than at two dimensions. When we commenced this calculation there were serious discrepancies between different estimates for the percolation threshold for the simple-cubic bond problem.[24–26] These discrepancies are large enough to cause substantial differences in exponent estimates, and are several orders of magnitude larger than the uncertainty in the 3D Ising model.[35] While writing up our results, we heard[36,37] that some very recent simulations improved this situation and we shall discuss these results in depth in our conclusion.

It does seem to be rather important to obtain a good understanding of the 3D critical behavior since many real systems with interesting percolation phenomena are three dimensional. One of the most interesting consequences of the uncertainty surrounding 3D percolation critical data is the possibility of a negative η estimate[18] in a physical dimension. η is the exponent that describes the critical behavior of the pair-correlation function $\mathcal{G}(r) \sim 1/r^{d-2+\eta}$ at distance r. Direct calculations of η for three dimensions have only been made from field theories; several different ones have been made and these disagree with each other.[10,16,19,30] However, since η is related to two other exponents via scaling relations, for example,

$$\gamma = \nu(2-\eta) , \tag{1.5}$$

estimates of η can be made from series expansion and Monte Carlo studies of γ and ν as well. One way to obtain ν from the series is via the hyperscaling relation $d\nu = 2-\alpha = 2\beta+\gamma$, and thus a reliable estimate of β in three dimensions is highly desirable. Most extant series expansion analyses of β have attempted to obtain β directly from a high-density $P(p)$ series.[20–22] The exception is Ref. 5 where β is calculated from the moment series but the systematic error here was large owing to the shortness of the series. In general, better convergence is to be expected from a low-density series but for 3D percolation the extant high-density series are considerably longer.[23] There is considerable spread of β estimates in the literature ranging from $\beta=0.34$ from the field

TABLE II. Bond-percolation thresholds for cubic lattices.

Method	Hypercubic	Hyper-bcc
	$D=2$	
Exact[a]	$\frac{1}{2}$	$\frac{1}{2}$
	$D=3$	
Previous series[b]	0.2479±0.0004	0.1795±0.0003
Monte Carlo[c]	0.248 65±0.000 13	
Monte Carlo[d]	0.2493±0.0002	
Monte Carlo[e]	0.2488 10±0.000 05	
Monte Carlo[f]	0.2488±0.0001	
This calculation	0.2488±0.0002	0.180 25±0.000 15
	$D=4$	
Previous series[g]	0.1600±0.0002	
Previous series[h]	0.161±0.0015	
Previous series[i]	0.1603±0.0002	
Monte Carlo[c]	0.160 13±0.000 12	
$1/\sigma$ expansion[j]	0.1533	
This calculation	0.160 05±0.000 15	
	$D=5$	
Previous series[g]	0.1181±0.0002	
Previous series[h]	0.118±0.001	
Previous series[i]	0.1182±0.0002	
$1/\sigma$ expansion[j]	0.1157	
This calculation	0.118 19±0.000 04	
	$D=6$	
Previous series[g]	0.0943±0.0002	
Previous series[h]	0.0941±0.0005	
Previous series[i]	0.094 075±0.0001	
$1/\sigma$ expansion[j]	0.093 30	
This calculation	0.094 20±0.0001	
	$D=7$	
Previous series[g]	0.0788±0.0002	
Previous series[h]	0.0786±0.0002	
Previous series[i]	0.078 62±0.000 03	
$1/\sigma$ expansion[j]	0.078 32	
This calculation	0.078 685±0.000 03	
	$D=8$	
Previous series[f]	0.067 70±0.000 05	
$1/\sigma$ expansion[j]	0.067 56	
This calculation	0.067 70±0.000 05	
	$D=9$	
Previous series[i]	0.059 50±0.000 05	
$1/\sigma$ expansion[j]	0.059 42	
This calculation	0.059 50±0.000 05	

[a]Reference 7.
[b]Reference 21.
[c]Reference 26.
[d]Reference 24.
[e]Reference 37.
[f]Reference 36.
[g]Reference 27.
[h]Reference 28.
[i]Reference 33.
[j]Reference 42.

theory.[16,30] to above ≈ 0.45 from some of the series calculations. Considerable spreading has also been observed between bond- and site-series estimates.[21] Thus, one of the motivations for the generation and analysis of the longer low-density moment series presented in this paper is reliable β (and hence η) estimate for three dimensions. Towards this end we have also carried out a comprehensive analysis of the Sykes-Wilkinson[23] high-density series.

For $d=4$ and 5 there have been some disagreements in the past between ϵ-expansion[30] and Monte Carlo[31,32] exponent values but these were mostly settled by the series results of Ref. 5 and the final version of the calculations of Grassberger.[26] (Slight discrepancies remained between the series and simulation threshold estimates at four dimensions and between the series and ϵ-expansion exponents at five dimensions.[5,26,30] Our new results reconcile both these inconsistencies.) These dimensions are close enough to the upper critical dimension to lead us to believe that the ϵ expansion exponent results are quite reliable, and our previous calculation in Ref. 5 confirmed this. It is, however, if considerable interest in the light of certain questions about other models to obtain critical exponents and thresholds in $d=4$ and 5 to as high an accuracy as possible. One example of such a question concerns the relation between the zero-temperature transition in the dilute spin glass[38] and the transition in other models. The identity or otherwise between the location of this transition and p_c was in some dispute until very recently. In order to demonstrate the separation of the transitions, accurate knowledge of both is required. Similar accurate knowledge of exponents for all the potential candidates (which includes percolation) for the universality class of the zero-temperature spin glass is also essential. To facilitate the making of such fine but important distinctions we further refine the exponent and threshold values that were given in Ref. 5.

The plan of our paper is as follows. A comprehensive summary of extant exponent and threshold values is given in Tables I and II, together with the conclusions from our analyses. In Sec. II we discuss the derivation of the expansions for all the moments of the percolation cluster-size distribution. The series are given in Table III. In Sec. III we present analyses of critical thresholds and exponents for $d>2$; comprehensive summaries of our results for $3\geq d\geq 5$ are presented in Tables IV and V. Section IV is devoted to the analysis of the amplitude ratios, with the results being displayed in Table VI. Conclusions and comparisons with other calculations are given in Sec. VI. Appendices are devoted to the mean-field free energy (as obtained on a Cayley tree) as a function of the field (including corrections to scaling) and to the site-bond generating function.

II. DERIVATION OF ARBITRARY MOMENTS OF THE CLUSTER-SIZE DISTRIBUTION FROM NO-FREE-END DIAGRAMS

As discussed elsewhere[39,40] it is useful to construct series using the tabulation of weights of only diagrams with no free ends (NFE). Here we obtain the transformation by which the free energy, F, for bond percolation as a function of field h can be obtained in terms of only NFE diagrams. Although we use the Potts model[41] to derive the transformation, the final results of (2.21) and (2.24b) are expressed in terms of cluster variables. The extension of these results to treat the site-bond generating function is described in Appendix B.

As is well-known,[1,2,41–44] the cluster-size distribution function can be obtained from the free energy of the $q\rightarrow 1$ Potts model, whose Hamiltonian we write as

$$H=-K\sum_{\langle x,x'\rangle}[\delta_{s(x),s(x')}-1]-h\sum_{x}[q\delta_{s(x),1}-1]\ , \tag{2.1}$$

where x labels sites, $\langle x,x'\rangle$ indicates that the sum is over pairs of nearest neighbors, $s(x)$ is a discrete (Potts) variable which can assume the values $1,2,\ldots,q$, and δ is the Kronecker δ. In the limit $q\rightarrow 1$ the free energy F is

$$\begin{aligned}F&\equiv\lim_{q\rightarrow 1}\frac{1}{N(q-1)}\ln \mathrm{Tr}\exp(-H)\\&=h+\sum_{n}W(n,p)\exp(-nh)\ ,\end{aligned} \tag{2.2}$$

where $W(n,p)$ is the average number of clusters per site having n sites. For $p<p_c$, when all the sites are in finite clusters, we have ($h\rightarrow 0$)

$$\frac{\partial F}{\partial h}=1-\sum_{n}nW(n,p)=0 \tag{2.3}$$

and for $h=0$ we write

$$\frac{\partial^j F}{\partial h^j}=(-1)^j\sum_{n}n^jW(n,p)\equiv(-1)^j\Gamma_j(p)\ ,\quad j>1\ . \tag{2.4}$$

Successive derivatives of the free energy with respect to h thus give the moments of the cluster-size distribution, whose critical behavior was given in Eq. (1.4).

We give here a prescription for a diagrammatic evaluation of $F(p,h)$ in powers of bond concentration p in terms of only NFE diagrams. To eliminate diagrams with free ends,[39] we consider $Z=\mathrm{Tr}\exp(-H)$, which we write as

$$\begin{aligned}Z=\mathrm{Tr}\Bigg[&\prod_{x}\{\exp[h(q\delta_{s(x),1}-1)]\rho(s(x))^z\}\\&\times\prod_{b}\left[1+\frac{1-p+p\delta_{s(x),s(x')}}{\rho(s(x))\rho(s(x'))}-1\right]\Bigg]\ ,\end{aligned} \tag{2.5}$$

where $p=1-\exp(-K)$, $\prod_b$ indicates a product over all nearest-neighbor bonds (x,x'), z is the coordination number of the pure lattice, and $\rho(s(x))$ is to be determined. We expand the product over bonds to get

$$\begin{aligned}Z&=\left[\mathrm{Tr}\left[\prod_{x}\exp[h(q\delta_{s(x),1}-1)]\rho(s(x))^z\right]\right]\\&\quad\times\left[1+\sum_{\Gamma}NW(\Gamma)Z(\Gamma)\right]\ ,\\Z&\equiv Z_1^N\left[1+\sum_{\Gamma}NW(\Gamma)Z(\Gamma)\right]\ ,\end{aligned} \tag{2.6}$$

where $W(\Gamma)$ is the number of times per site a diagram (consisting of a nonempty set of bonds) topologically equivalent to Γ can be formed on the lattice of N sites (with $N\rightarrow\infty$), the sum is over all topologically inequivalent diagrams Γ, and

$$Z(\Gamma)=\operatorname{Tr}_{\Gamma}\left[\prod_{x\in\Gamma}\{\exp[h(q\delta_{s(x),1}-1)]\rho(s(x))^{z}\}\prod_{b\in\Gamma}\left[\frac{(1-p+p\delta_{s(x),s(x')})}{\rho(s(x))\rho(s(x'))}-1\right]\right]Z_1^{-n_s(\Gamma)}, \tag{2.7}$$

where $n_s(\Gamma)$ is the number of sites in the diagram Γ and Tr_Γ indicates a trace over all $s(x)$ with $x\in\Gamma$. We now determine $\rho(s(x))$ so that for diagrams γ with free ends, $Z(\gamma)=0$. For such a diagram some site x' appears in only one bond and we require that the trace over such an $s(x')$ should vanish. From this requirement we find that $\rho(s(x))$ satisfies

$$\rho(s(x))=\frac{\operatorname{Tr}_{s(x')}\exp[h(q\delta_{s(x'),1}-1)]\rho(s(x'))^{\sigma}(1-p+p\delta_{s(x),s(x')})}{\operatorname{Tr}_{s(x')}\exp[h(q\delta_{s(x'),1}-1)]\rho(s(x'))^{z}}, \tag{2.8}$$

where $\sigma=z-1$. We assume a solution to (2.8) in the form

$$\rho(s(x))=A\exp[B(q\delta_{s(x),1}-1)]. \tag{2.9}$$

Physically, one can identify B as an effective field which takes account of free ends. Substituting the ansatz (2.9) into (2.8) we get the conditions

$$\begin{aligned}A^2\exp[B(q-1)]&=\frac{\{\exp[(h+\sigma B)(q-1)]+(q-1)(1-p)\exp[-(h+\sigma B)]\}}{\{\exp[(h+zB)(q-1)]+(q-1)\exp[-(h+zB)]\}},\\ A^2\exp[-B]&=\frac{\{(1-p)\exp[(h+\sigma B)(q-1)]+\exp[-(h+\sigma B)][1+(1-p)(q-2)]\}}{\{\exp[(h+zB)(q-1)]+(q-1)\exp[-(h+zB)]\}},\end{aligned} \tag{2.10}$$

from the cases $s(x)=1$ and $s(x)\neq 1$, respectively. In the limit $q\to 1$ we find that B is the solution to

$$\exp[-B]=1-p+p\exp[-(h+\sigma B)], \tag{2.11}$$

so that B can be obtained exactly up to any desired order in h:

$$B=\Sigma_k B_k h^k. \tag{2.12a}$$

To order h^2 we have

$$B=\frac{ph}{1-\sigma p}-\frac{1}{2}\frac{p(1-p)h^2}{(1-\sigma p)^3} \tag{2.12b}$$

and, in general, B_k will diverge for $p\to p_c=\sigma^{-1}$ as $(1-\sigma p)^{2k-1}$ corresponding to the mean-field value of the gap exponent $\beta+\gamma=2$. Solving Eq. (2.10) to order $(q-1)$ for A we get $A=1+(q-1)a$ with

$$a=-\tfrac{1}{2}\{2B+\exp[-(h+zB)]-(1-p)\exp[-(h+\sigma B)]\}, \tag{2.13}$$

so that a can likewise be expanded as a power series in h up to any desired order.

Now we substitute the solution for $\rho(s(x))$ into (2.7). In so doing, note that $\rho(s(x))=1$ for $q=1$ so that $Z(\Gamma)$ is of order $(q-1)$. In fact, if Γ consists of k disjoint clusters, $Z(\Gamma)$ is of order $(q-1)^k$. Thus, the sum in (2.6) can be confined to topologically inequivalent connected NFE clusters, which we indicate by Γ: NFE. Also, $Z\to 1$ as $q\to 1$. Thus, we have

$$\begin{aligned}Z&=Z_1^N\left[1+\sum_{\Gamma:\mathrm{NFE}}{}'NW(\Gamma)Z(\Gamma)\right]\\ &\equiv 1+N(q-1)F+O(q-1)^2.\end{aligned} \tag{2.14}$$

For a lattice with no loops, there are no terms in the summation in (2.14). Thus, the first term represents the exact solution for a Cayley tree of coordination number z. Explicitly the single-site partition function Z_1 is

$$\begin{aligned}Z_1&=\operatorname{Tr}_{s(x)}A^z\exp[(h+zB)(q\delta_{s(x),1}-1)]\\ &=A^z\{\exp[(q-1)(h+zB)]+(q-1)\exp[-(h+zB)]\}.\end{aligned} \tag{2.15}$$

Using (2.13) we have, for $q\to 1$

$$\begin{aligned}Z_1&=1+(q-1)\left[h-\frac{z-2}{2}\exp[-(h+zB)]+\frac{z}{2}(1-p)\exp[-(h+\sigma B)]\right]\\ &\equiv 1+(q-1)F_{\mathrm{CT}},\end{aligned} \tag{2.16}$$

where F_{CT} is the free energy for the Cayley tree, in terms of which

$$F=F_{\mathrm{CT}}+\lim_{q\to 1}\sum_{\Gamma:\mathrm{NFE}}W(\Gamma)Z(\Gamma)/(q-1). \tag{2.17}$$

In Appendix A we use a recursive method[42] to obtain the free energy for the Cayley tree with *the leading analytic corrections to scaling,*

$$F_{\rm CT}=\frac{\sigma-1}{2\sigma}-\frac{\sigma+1}{2}(p-p_c)+\frac{(\sigma+1)(p-p_c)^3\sigma^4}{3(\sigma-1)^2}\left[1+\frac{3y}{2}-(1+y)^{3/2}\right]$$
$$+\frac{(\sigma+1)(p-p_c)^4\sigma^5\{-2\sigma+1-(4\sigma+1)y/2+(1+y)^{1/2}[2\sigma-1+y(\sigma+1)]-\frac{1}{4}y^2(\sigma^2+5\sigma+1)/(\sigma+1)\}}{3(\sigma-1)^3} \tag{2.18}$$

where $y=2(\sigma-1)h/[\sigma^3(p-p_c)^2]$. The leading terms [up to order $(p-p_c)^3$] in (2.18) were previously given within mean-field theory.[43,44] The correction terms of order $(p-p_c)^4$ are given here for the first time. Note that although we cannot give the general solution for the percolation free energy *in a field,* we can give it correct to any arbitrary order in corrections to scaling. Here, for instance, we give the full field dependence of the leading and first correction terms.

Now we manipulate $Z(\Gamma)$ into a convenient form. For this purpose recall one of the definitions of the cumulant, indicated by the subscript c:

$$Y_c(\Gamma)=\sum_{\gamma\in\Gamma}(-1)^{n_b(\gamma)-n_b(\Gamma)}Y(\gamma)\ , \tag{2.19}$$

where the sum is over all sets of one or more bonds γ (connected or not) which are subsets of Γ, including $\gamma=\Gamma$. There are $2^{n_b(\Gamma)}-1$ such subsets. To use this relation we expand the product over bonds in (2.7) associating with the factor -1 a vacant bond and with the factor

$$[1-p+p\delta_{s(x),s(x')}]/\rho(s(x))\rho(s(x'))$$

an occupied bond. The expansion of this product therefore yields $2^{n_b(\Gamma)}$ terms, which except for the term with no occupied bonds, are in a one-to-one correspondence with the set of subdiagrams γ of Γ as in (2.19). We write the result as

$$Z(\Gamma)=\sum_{\gamma}(-1)^{n_b(\Gamma)-n_b(\gamma)}\left[Z_1^{-n_s(\gamma)}\operatorname*{Tr}_{\gamma}\prod_{x\in\gamma}\exp[h(q\delta_{s(x),1}-1)]\rho(s(x))^z\right]\left[-1+\prod_{b\in\gamma}\frac{(1-p+p\delta_{s(x),s(x')})}{[\rho(s(x))\rho(s(x'))]}\right] \tag{2.20a}$$

$$\equiv(q-1)\sum_{\gamma}(-)^{n_b(\Gamma)-n_b(\gamma)}Y(\gamma)=(q-1)Y_c(\Gamma),\quad q\to1\ . \tag{2.20b}$$

This equation defines $Y(\Gamma)$ to be the product of the factors in large parentheses in Eq. (2.20a). Thus,

$$F=F_{\rm CT}+\sum_{\Gamma:\rm NFE}W(\Gamma)Y_c(\Gamma)\ . \tag{2.21}$$

We now write $Y(\Gamma)$ in terms of bond variables. In the limit $q\to1$, $Z_1\to1$ and $A\to1$, so that in this limit we may write

$$(q-1)Y(\Gamma)=-1+\frac{A^{zn_s(\Gamma)-2n_b(\Gamma)}}{Z_1^{n_s(\Gamma)}}\operatorname*{Tr}_{\Gamma}\prod_{x\in\Gamma}\exp\{(q\delta_{s(x),1}-1)[h+zB-z_x(\Gamma)B]\}\prod_{b\in\Gamma}(1-p+p\delta_{s(x),s(x')})$$
$$=(A^{zn_s(\Gamma)-2n_b(\Gamma)}-1)+(1-Z_1^{n_s(\Gamma)})-1+\operatorname*{Tr}_{\Gamma}\prod_{x\in\Gamma}\exp\{(q\delta_{s(x),1}-1)[h+zB-z_x(\Gamma)B]\}$$
$$\times\prod_{b\in\Gamma}(1-p+p\delta_{s(x),s(x')})\ , \tag{2.22}$$

where $z_x(\Gamma)$ is the number of bonds intersecting site x in the diagram Γ. The trace here is that of a Potts model for a cluster Γ in an inhomogeneous field $\tilde{h}(x)$, where

$$\tilde{h}(x)=h+zB-z_x(\Gamma)B\ . \tag{2.23}$$

We now evaluate this trace in terms of a sum over all possible clusters $C(\Gamma)$ of bonds of Γ such that each site is directly or indirectly connected by occupied bonds with all other sites in the cluster. In this context an isolated site is considered to be a cluster. This type of evaluation is discussed in detail in Ref. 44. Thus we find

$$Y(\Gamma)=\left[\frac{zn_s(\Gamma)}{2}-n_b(\Gamma)\right]\{-2B-\exp[-(h+zB)]+(1-p)\exp[-(h+\sigma B)]\}$$
$$-n_s(\Gamma)\left[h-\frac{(z-2)}{2}\exp[-(h+zB)]+\frac{z}{2}(1-p)\exp[-(h+\sigma B)]\right]$$
$$+\sum_{C(\Gamma)}P(C;\Gamma)\left[\exp\left[-\sum_{x\in C}\tilde{h}(x)\right]+\sum_{x\in C}\tilde{h}(x)\right] \tag{2.24a}$$

$$=[n_b(\Gamma)-n_s(\Gamma)]\exp[-(h+zB)]-(1-p)n_b(\Gamma)\exp[-(h+\sigma B)]+\sum_{C\in\Gamma}P(C;\Gamma)\exp\left[-\sum_{x\in C}\tilde{h}(x)\right]\ , \tag{2.24b}$$

where $\tilde{h}(x)$ is given in (2.23). Here $P(C;\Gamma)$ is the probability that a cluster of sites C occur when the system is considered to be the set of bonds Γ and is given by

$$P(C;\Gamma)=p^{n_b(C)}(1-p)^{n_t(C;\Gamma)} ,$$

where $n_t(\Gamma)$ is the number of perimeter bonds which is in Γ. [For example, see Eq. (2.26) below.] Note that a check on (2.24) is to evaluate it for diagrams γ with one or more free ends and obtain $Y_c(\gamma)=0$.

To summarize the procedure, we evaluate $F(h)$ to any desired order in h in terms of the sum over NFE diagrams in (2.17), where $Y_c(\Gamma)$ is the cumulant value of $Y(\Gamma)$. For any Γ, $Y(\Gamma)$, is given by (2.24) and $Y_c(\Gamma)$ is obtained recursively from $Y(\Gamma)$ via

$$Y_c(\Gamma)=Y(\Gamma)-\sum_{\gamma\in\Gamma} Y_c(\gamma) . \tag{2.25}$$

To illustrate (2.24b) we evaluate it for the case when Γ is the cluster shown in Fig. 1(a), where $n_s(\Gamma)=3$ and $n_b(\Gamma)=2$. Of course, since this cluster has free ends, $Y_c(\Gamma)$ will be zero. We get

$$\begin{aligned} Y(\Gamma)=&(2-3)\exp[-(h+zB)]-(1-p)(2)\exp[-(h+\sigma B)] \\ &+(1-p)\exp[-(h+zB-B)]+(1-p)^2\exp[-(h+zB-2B)] \\ &+(1-p)\exp[-(h+zB-B)]+p(1-p)\exp[-2(h+zB)+3B] \\ &+p(1-p)\exp[-2(h+zB)+3B]+p^2\exp[-3(h+zB)+4B] . \end{aligned} \tag{2.26}$$

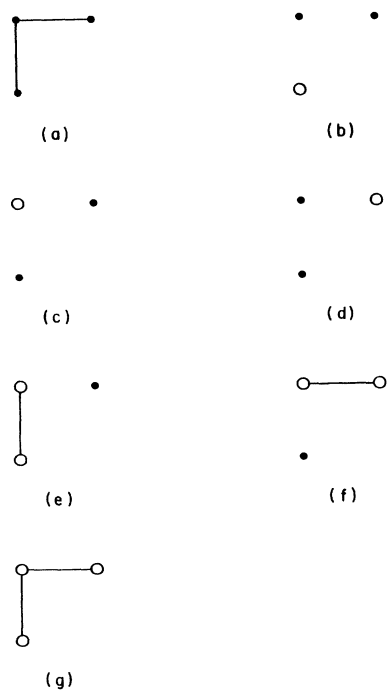

FIG. 1. (a) shows the cluster for which Eq. (2.26) is constructed. This cluster has three sites and two bonds. (b)–(g) show subclusters, C, of sites (indicated by open circles) which can be formed on the cluster shown in (a). Note that a cluster is defined by the presence of bonds needed to connect the sites of the cluster and by the absence of perimeter bonds. Bonds not intersecting a site of the cluster can be either occupied or not.

The last six terms in Eq. (2.26) come from the clusters shown in Figs. 1(b)–(g), respectively. Repeated use of (2.11) shows that this is indeed zero. The simplest nonzero contribution comes from a square, for which $W(\Gamma)=d(d-1)/2$. Here we find

$$\begin{aligned} Z(\Gamma)=&Y(\Gamma) \\ =&p^4\exp[-4(h+\sigma B-B)] \\ &\times\{5-4p-4(1-p)\exp[-(h+\sigma B-B)]\} . \end{aligned} \tag{2.27}$$

Note that this result contains only powers of p at least as large as the number of bonds in the diagram. That is a general property of the cumulants. Thus, to obtain a series up to order, say p^{15}, we need to sum the contributions of all NFE diagrams with up to, and including, 15 bonds. The tabulation of the relevant $W(\Gamma)$ is described elsewhere.[39] Fortunately, the list of NFE diagrams is not very large. The calculation of cumulants, requires subtracting from a given NFE diagram the contributions from all NFE subdiagrams according to Eq. (2.25). A check on the procedure is that, whereas $Y(\Gamma)$ may contain lower powers of p, when the cumulant subtraction is performed, the resulting $Z(\Gamma)$ has no contribution with powers of p lower than $p^{n_b(\Gamma)}$.

The series are given in Table III. We give the first three moments as rational fractions but were unable to deduce the rational form for the highest moments. The two-dimensional $S(p)$ series agrees with previous calculations and the three-dimensional one agrees to 14th order with the corresponding series of Sykes and Wilkinson.[23] The calculation of identical elements of the series by two

TABLE III. Series coefficients for Γ_j, where $\Gamma_j = 1 + \sum_{m,n} a_j(m,n) p^m d^n$.

m	n	$a_j(m,n)\times 15$	m	n	$a_j(m,n)\times 15$
		Moment no. 3			
1	1	30	2	1	−30
2	2	60	3	1	30
3	2	−120	3	3	120
4	1	120	4	2	30
4	3	−360	4	4	240
5	1	−510	5	2	900
5	3	120	5	4	−960
5	5	480	6	1	−1740
6	2	930	6	3	1680
6	4	600	6	5	−2400
6	6	960	7	1	13 260
7	2	−26 970	7	3	11 820
7	4	3360	7	5	2400
7	6	−5760	7	7	1920
8	1	89 970	8	2	−125 460
8	3	14 940	8	4	15 300
8	5	6720	8	6	8160
8	7	−13 440	8	8	3840
9	1	−663 520	9	2	1634 810
9	3	−1297 340	9	4	297 160
9	5	14 520	9	6	12 480
9	7	24 960	9	8	−30 720
9	9	7680	10	1	−6953 640
10	2	12 959 570	10	3	−6262 300
10	4	−279 320	10	5	502 600
10	6	−3360	10	7	19 200
10	8	71 040	10	9	−69 120
10	10	15 360	11	1	45 170 190
11	2	−130 083 820	11	3	135 168 100
11	4	−58 203 440	11	5	7063 400
11	6	874 080	11	7	−72 960
11	8	15 360	11	9	192 000
11	10	−153 600	11	11	30 720
12	1	732 007 250	12	2	−1632 340 205
12	3	1196 154 625	12	4	−277 847 700
12	5	−31 538 300	12	6	12 079 880
12	7	1587 200	12	8	−279 360
12	9	−46 080	12	10	499 200
12	11	−337 920	12	12	61 440
13	1	−4002 430 140	13	2	13 170 655 275
13	3	−16 560 801 405	13	4	9826 966 040
13	5	−2644 473 740	13	6	186 873 440
13	7	20 648000	13	8	3056 000
13	9	−816 000	13	10	−322 560
13	11	1259 520	13	12	−737 280
13	13	122 880	14	1	−98 173 988 490
14	2	248 113 345 025	14	3	−228 622 164 705
14	4	91 499 593 880	14	5	−11 234 076 680
14	6	−1952 641 400	14	7	330 117 680
14	8	35 151 040	14	9	6291 840
14	10	−2088 960	14	11	−1290 240
14	12	3102 720	14	13	−1597 440
14	14	245 760	15	1	463 111 949 890
15	2	−1691 377 838 763	15	3	2442 735 580 335
15	4	−1778 594 306 480	15	5	682 114 561 680
15	6	−123 841 537 192	15	7	5198 261 920
15	8	584 938 880	15	9	59 217 280
15	10	13 795 840	15	11	−4869 120
15	12	−4300 800	15	13	7495 680
15	14	−3440 640	15	15	491 520
		Moment no. 4			
1	1	90	2	1	−180
2	2	360	3	1	330
3	2	−1260	3	3	1200
4	1	810	4	2	1710
4	3	−5760	4	4	3600
5	1	−7290	5	2	10 980
5	3	8280	5	4	−21 600
5	5	10 080	6	1	−11 610
6	2	−20 430	6	3	40 500
6	4	37 200	6	5	−72 000
6	6	26 880	7	1	240 120
7	2	−436 590	7	3	83 340
7	4	115 200	7	5	151 200
7	6	−221 760	7	7	69 120
8	1	1108 530	8	2	−817 110
8	3	−913 860	8	4	261 720
8	5	273 600	8	6	560 160
8	7	−645 120	8	8	172 800
9	1	−15 798 120	9	2	37 170 990

TABLE III. (*Continued*).

m	n	$a_j(m,n)\times 15$	m	n	$a_j(m,n)\times 15$
		Moment no. 4			
9	3	−25 944 420	9	4	3158 520
9	5	360 720	9	6	505 920
9	7	1921 920	9	8	−1797 120
9	9	422 400	10	1	−119 721 960
10	2	174 566 880	10	3	−6701 100
10	4	−65 770 200	10	5	15 228 240
10	6	−397 440	10	7	423 360
10	8	6197 760	10	9	−4838 400
10	10	1013 760	11	1	1354 091 130
11	2	−3783 729 000	11	3	3665 935 020
11	4	−1294 704 720	11	5	8844 720
11	6	47 605 440	11	7	−4700 160
11	8	−2073 600	11	9	19 008 000
11	10	−12 672 000	11	11	2396 160
12	1	16 289 833 980	12	2	−31 971 608 865
12	3	15 844 995 285	12	4	2977 105 860
12	5	−3516 130 860	12	6	250 755 120
12	7	131 712 960	12	8	−20 286 720
12	9	−15 475 200	12	10	55 948 800
12	11	−32 440 320	12	12	5591 040
13	1	−146 826 349 920	13	2	472 126 082 055
13	3	−567 323 094 585	13	4	304 988 652 480
13	5	−61 733 381 580	13	6	−2412 785 040
13	7	877 344 960	13	8	349 313 280
13	9	−66 562 560	13	10	−69 811 200
13	11	159 160 320	13	12	−81 469 440
13	13	12 902 400	14	1	−2657 401 491 600
14	2	6215 832 272 295	14	3	−4775 591 977 845
14	4	980 856 638 070	14	5	410 670 039 420
14	6	−180 630 071 400	14	7	3203 685 120
14	8	2325 612 480	14	9	915 536 640
14	10	−185 448 960	14	11	−262 978 560
14	12	439 971 840	14	13	−201 277 440
14	14	29 491 200	15	1	20 164 588 285 410
15	2	−72 234 114 387 489	15	3	100 953 857 842 275
15	4	−69 137 430 756 810	15	5	23 245 240 389 780
15	6	−2814 562 847 976	15	7	−205 144 839 360
15	8	20 346 443 520	15	9	5404 512 000
15	10	2396 843 520	15	11	−448 404 480
15	12	−896 532 480	15	13	1186 897 920
15	14	−490 291 200	15	15	66 846 720

m	n	$a_j(m,n)\times 15$	m	n	$a_j(m,n)\times 15$
		Moment no. 5			
1	1	210	2	1	−750
2	2	1500	3	1	2250
3	2	−8400	3	3	7800
4	1	3540	4	2	21 570
4	3	−55 800	4	4	33 600
5	1	−69 450	5	2	84 300
5	3	147 600	5	4	−285 600
5	5	127 680	6	1	−2160
6	2	−499 530	6	3	470 880
6	4	837 000	6	5	−1243 200
6	6	443 520	7	1	2917 380
7	2	−4473 150	7	3	−868 980
7	4	1711 200	7	5	4120 800
7	6	−4838 400	7	7	1440 000
8	1	8606 490	8	2	5222 580
8	3	−21 720 300	8	4	−1658 820
8	5	4320 000	8	6	18 144 000
8	7	−17 337 600	8	8	4435 200
9	1	−255 478 480	9	2	564 609 590
9	3	−328 364 180	9	4	−4130 360
9	5	−8947 080	9	6	4462 080
9	7	73 059 840	9	8	−58 291 200
9	9	13 094 400	10	1	−1421 516 760
10	2	1139 685 890	10	3	1748 868 620
10	4	−1720 844 960	10	5	213 101 080
10	6	−53 889600	10	7	−30 105 600
10	8	273 657 600	10	9	−186 278 400
10	10	37 340 160	11	1	27 519 547 770
11	2	−73 773 159 820	11	3	64 956 131 620
11	4	−16 271 480 600	11	5	−3623 573 800
11	6	1214 642 400	11	7	−254 136 960
11	8	−266 250 240	11	9	965 952 000
11	10	−571 084 800	11	11	103 434 240
12	1	259 593 835 190	12	2	−411 596 664 315
12	3	20 838 492 435	12	4	225 879 256 940
12	5	−94 830 599 220	12	6	−4247 850 920
12	7	4921 609 600	12	8	−972 120 960
12	9	−1419 494 400	12	10	3245 299 200
12	11	−1691 289 600	12	12	279 552 000
13	1	−3632 252 403 060	13	2	11 335 071 490 065
13	3	−12 846 686 272 615	13	4	6009 658 033 840

TABLE III. (*Continued*).

m	n	$a_j(m,n)\times 15$	m	n	$a_j(m,n)\times 15$
		Moment no. 5			
13	5	−646 761 418 260	13	6	−236 148 923 840
13	7	2762 222 560	13	8	17 384 224 000
13	9	−3119 927 040	13	10	−6241 152 000
13	11	10 458 624 000	13	12	−4864 204 800
13	13	739 737 600	14	1	−52 369 225 586 130
14	2	109 320 465 179 555	14	3	−58 121 143 837 135
14	4	−16 435 293 886 140	14	5	22 859 267 935 680
14	6	−4913 562 611 080	14	7	−419 852 823 440
14	8	34 366 288 640	14	9	57 078 746 880
14	10	−8 357 583 360	14	11	−24 550 563 840
14	12	32 529 070 080	14	13	−13 642 137 600
14	14	1921 843 200	15	1	588 660 984 524 710
15	2	−2060 881 406 952 081	15	3	2766 952 632 888 185
15	4	−1749 807 454 011 980	15	5	480 982 412 703 880
15	6	−11 683 670 714 744	15	7	−14 024 051 745 280
15	8	−464 063 221 760	15	9	126 823 015 680
15	10	178 857 638 400	15	11	−17 173 017 600
15	12	−89 492 889 600	15	13	98 122 752 000
15	14	−37 434 163 200	15	15	4913 233 920

m	n	$a_j(m,n)$	m	n	$a_j(m,n)$
		Moment no. 6			
1	1	$0.300\,000\,000\,000\,000\,0000\times 10^{2}$	2	1	$-0.180\,000\,000\,000\,000\,0000\times 10^{3}$
2	2	$0.360\,000\,000\,000\,000\,0000\times 10^{3}$	3	1	$0.830\,000\,000\,000\,000\,0000\times 10^{3}$
3	2	$-0.306\,000\,000\,000\,000\,0000\times 10^{4}$	3	3	$0.280\,000\,000\,000\,000\,0000\times 10^{4}$
4	1	$0.690\,000\,000\,000\,000\,0000\times 10^{3}$	4	2	$0.123\,900\,000\,000\,000\,0000\times 10^{5}$
4	3	$-0.285\,600\,000\,000\,000\,0000\times 10^{5}$	4	4	$0.168\,000\,000\,000\,000\,0000\times 10^{5}$
5	1	$-0.369\,420\,000\,000\,000\,0000\times 10^{5}$	5	2	$0.335\,400\,000\,000\,000\,0000\times 10^{5}$
5	3	$0.116\,160\,000\,000\,000\,0000\times 10^{6}$	5	4	$-0.194\,880\,000\,000\,000\,0000\times 10^{6}$
5	5	$0.846\,720\,000\,000\,000\times 10^{5}$	6	1	$0.601\,700\,000\,000\,000\,0000\times 10^{5}$
6	2	$-0.440\,570\,000\,000\,000\,0000\times 10^{6}$	6	3	$0.254\,140\,000\,000\,000\,0000\times 10^{6}$
6	4	$0.842\,960\,000\,000\,000\,0000\times 10^{6}$	6	5	$-0.108\,864\,000\,000\,000\,0000\times 10^{7}$
6	6	$0.376\,320\,000\,000\,000\,0000\times 10^{6}$	7	1	$0.196\,404\,000\,000\,000\,0000\times 10^{7}$
7	2	$-0.232\,245\,000\,000\,000\,0000\times 10^{7}$	7	3	$-0.202\,194\,000\,000\,000\,0000\times 10^{7}$
7	4	$0.103\,464\,000\,000\,000\,0000\times 10^{7}$	7	5	$0.511\,392\,000\,000\,000\,0000\times 10^{7}$
7	6	$-0.528\,192\,000\,000\,000\,0000\times 10^{7}$	7	7	$0.152\,064\,000\,000\,000\,0000\times 10^{7}$
8	1	$0.373\,365\,000\,000\,000\,0000\times 10^{7}$	8	2	$0.114\,881\,700\,000\,000\,0000\times 10^{8}$
8	3	$0.181\,049\,400\,000\,000\,0000\times 10^{8}$	8	4	$-0.848\,064\,000\,000\,000\,0000\times 10^{7}$
8	5	$0.164\,640\,000\,000\,000\,0000\times 10^{7}$	8	6	$0.270\,883\,200\,000\,000\,0000\times 10^{8}$
8	7	$-0.230\,630\,400\,000\,000\,0000\times 10^{8}$	8	8	$0.570\,240\,000\,000\,000\,0000\times 10^{7}$

m	n	$a_j(m,n)$	m	n	$a_j(m,n)$
		Moment no. 6			
9	1	$-0.238\,236\,407\,702\,5547\times 10^{9}$	9	2	$0.502\,923\,192\,801\,4706\times 10^{9}$
9	3	$-0.252\,222\,746\,404\,8769\times 10^{9}$	9	4	$-0.175\,329\,048\,573\,4223\times 10^{8}$
9	5	$-0.390\,540\,638\,366\,9672\times 10^{8}$	9	6	$-0.122\,080\,000\,000\,0000\times 10^{8}$
9	7	$0.128\,970\,240\,000\,0000\times 10^{9}$	9	8	$-0.927\,590\,400\,000\,0000\times 10^{8}$
9	9	$0.201\,344\,000\,000\,0000\times 10^{8}$	10	1	$-0.858\,679\,512\,013\,8972\times 10^{9}$
10	2	$-0.529\,098\,359\,916\,2078\times 10^{9}$	10	3	$0.344\,137\,931\,581\,3477\times 10^{10}$
10	4	$-0.230\,422\,683\,181\,0889\times 10^{10}$	10	5	$0.291\,753\,135\,912\,2567\times 10^{9}$
10	6	$-0.180\,023\,871\,984\,7403\times 10^{9}$	10	7	$-0.142\,961\,280\,000\,0000\times 10^{9}$
10	8	$0.563\,466\,240\,000\,0000\times 10^{9}$	10	9	$-0.349\,240\,320\,000\,0000\times 10^{9}$
10	10	$0.676\,515\,840\,000\,0000\times 10^{8}$	11	1	$0.311\,335\,749\,423\,0210\times 10^{11}$
11	2	$-0.791\,134\,919\,864\,2565\times 10^{11}$	11	3	$0.604\,417\,249\,716\,9751\times 10^{11}$
11	4	$-0.479\,467\,598\,822\,0050\times 10^{10}$	11	5	$-0.957\,760\,510\,987\,0923\times 10^{10}$
11	6	$0.233\,056\,031\,585\,3594\times 10^{10}$	11	7	$-0.739\,026\,175\,336\,5751\times 10^{9}$
11	8	$-0.947\,566\,080\,000\,0000\times 10^{9}$	11	9	$0.229\,388\,544\,000\,0000\times 10^{10}$
11	10	$-0.124\,540\,416\,000\,0000\times 10^{10}$	11	11	$0.218\,050\,560\,000\,0000\times 10^{9}$
12	1	$0.232\,755\,068\,577\,2284\times 10^{12}$	12	2	$-0.242\,139\,814\,198\,9668\times 10^{12}$
12	3	$-0.266\,963\,081\,224\,4454\times 10^{12}$	12	4	$0.395\,599\,144\,948\,6545\times 10^{12}$
12	5	$-0.100\,502\,217924\,6134\times 10^{12}$	12	6	$-0.275\,009\,900\,898\,2054\times 10^{11}$
12	7	$0.110\,477\,522\,566\,5259\times 10^{11}$	12	8	$-0.249\,911\,726\,468\,9272\times 10^{10}$
12	9	$-0.503\,495\,424\,000\,0000\times 10^{10}$	12	10	$0.880\,346\,368\,000\,0000\times 10^{10}$
12	11	$-0.424\,359\,936\,000\,0000\times 10^{10}$	12	12	$0.678\,379\,520\,000\,0000\times 10^{9}$
13	1	$-0.499\,770\,532\,345\,4674\times 10^{13}$	13	2	$0.150\,613\,499\,980\,1210\times 10^{14}$
13	3	$-0.158\,935\,286\,204\,5417\times 10^{14}$	13	4	$0.607\,878\,850\,129\,6894\times 10^{13}$
13	5	$0.250\,614\,872\,766\,3956\times 10^{12}$	13	6	$-0.485\,727\,625\,183\,3799\times 10^{12}$
13	7	$-0.424\,746\,038\,034\,9541\times 10^{11}$	13	8	$0.379\,349\,083\,415\,7435\times 10^{11}$
13	9	$-0.605\,824\,329\,125\,1635\times 10^{10}$	13	10	$-0.234\,693\,888\,000\,0000\times 10^{11}$
13	11	$0.321\,388\,953\,600\,0000\times 10^{11}$	13	12	$-0.139\,105\,075\,200\,0000\times 10^{11}$
13	13	$0.204\,718\,080\,000\,0000\times 10^{10}$	14	1	$-0.593\,597\,014\,784\,2083\times 10^{14}$
14	2	$0.104\,243\,959\,925\,1513\times 10^{15}$	14	3	$-0.140\,037\,643\,289\,0103\times 10^{14}$
14	4	$-0.665\,661\,561\,017\,5368\times 10^{14}$	14	5	$0.419\,401\,885\,130\,8719\times 10^{14}$
14	6	$-0.455\,974\,778\,686\,6154\times 10^{13}$	14	7	$-0.190\,427\,830\,667\,2765\times 10^{13}$
14	8	$0.154\,269\,841\,988\,2610\times 10^{12}$	14	9	$0.837\,833\,131\,421\,4818\times 10^{11}$
14	10	$-0.302\,839\,525\,447\,0732\times 10^{10}$	14	11	$-0.998\,470\,809\,600\,0000\times 10^{11}$
14	12	$0.112\,407\,859\,200\,0000\times 10^{12}$	14	13	$-0.441\,021\,235\,200\,0000\times 10^{11}$
14	14	$0.601\,620\,480\,000\,0000\times 10^{10}$	15	1	$0.953\,777\,355\,819\,7888\times 10^{15}$
15	2	$-0.325\,381\,962\,470\,7913\times 10^{16}$	15	3	$0.416\,772\,855\,301\,4512\times 10^{16}$
15	4	$-0.238\,035\,283\,593\,9481\times 10^{16}$	15	5	$0.465\,928\,659\,629\,0533\times 10^{15}$
15	6	$0.742\,406\,062\,985\,5687\times 10^{14}$	15	7	$-0.214\,388\,241\,960\,2284\times 10^{14}$
15	8	$-0.800\,521\,936\,625\,9778\times 10^{13}$	15	9	$0.203\,699\,873\,897\,4247\times 10^{13}$
15	10	$-0.375\,162\,849\,399\,6222\times 10^{11}$	15	11	$0.778\,840\,564\,533\,2875\times 10^{11}$
15	12	$-0.396\,313\,415\,680\,0000\times 10^{12}$	15	13	$0.378\,819\,051\,520\,0000\times 10^{12}$
15	14	$-0.135\,815\,823\,360\,0000\times 10^{12}$	15	15	$0.172\,731\,924\,480\,0000\times 10^{11}$

TABLE III. (*Continued*).

m	n	$a_j(m,n)$	m	n	$a_j(m,n)$	m	n	$a_j(m,n)$	m	n	$a_j(m,n)$
		Moment no. 7						Moment no. 7			
1	1	$0.620\,000\,000\,000\,0000\times10^{2}$	2	1	$-0.602\,000\,000\,000\,0000\times10^{3}$	11	6	$0.103\,586\,624\,365\,9423\times10^{12}$	11	7	$-0.285\,147\,868\,755\,3173\times10^{11}$
2	2	$0.120\,400\,000\,000\,0000\times10^{4}$	3	1	$0.410\,200\,000\,000\,0000\times10^{4}$	11	8	$-0.341\,675\,089\,920\,0000\times10^{11}$	11	9	$0.650\,355\,763\,200\,0000\times10^{11}$
3	2	$-0.150\,080\,000\,000\,0000\times10^{5}$	3	3	$0.136\,080\,000\,000\,0000\times10^{5}$	11	10	$-0.331\,390\,259\,200\,0000\times10^{11}$	11	11	$0.564\,657\,766\,400\,0000\times10^{10}$
4	1	$0.248\,000\,000\,000\,0000\times10^{3}$	4	2	$0.887\,220\,000\,000\,0000\times10^{5}$	12	1	$0.275\,526\,937\,742\,7924\times10^{13}$	12	2	$-0.638\,267\,421\,117\,3243\times10^{12}$
4	3	$-0.192\,024\,000\,000\,0000\times10^{6}$	4	4	$0.111\,216\,000\,000\,0000\times10^{6}$	12	3	$-0.765\,097\,629\,805\,5031\times10^{13}$	12	4	$0.646\,148\,652\,870\,0394\times10^{13}$
5	1	$-0.267\,526\,000\,000\,0000\times10^{6}$	5	2	$0.161\,420\,000\,000\,0000\times10^{6}$	12	5	$0.499\,703\,638\,268\,3234\times10^{12}$	12	6	$-0.196\,844\,153\,752\,5116\times10^{13}$
5	3	$0.111\,008\,800\,000\,0000\times10^{7}$	5	4	$-0.171\,494\,400\,000\,0000\times10^{7}$	12	7	$0.685\,388\,846\,012\,2726\times10^{12}$	12	8	$-0.125\,025\,954\,349\,4412\times10^{12}$
5	5	$0.730\,464\,000\,000\,0000\times10^{6}$	6	1	$0.948\,344\,000\,000\,0000\times10^{6}$	12	9	$-0.194\,569\,503\,744\,0000\times10^{12}$	12	10	$0.284\,592\,788\,480\,0000\times10^{12}$
6	2	$-0.461\,910\,200\,000\,0000\times10^{7}$	6	3	$0.150\,975\,200\,000\,0000\times10^{7}$	12	11	$-0.129\,271\,926\,784\,0000\times10^{12}$	12	12	$0.201\,120890\,880\,0000\times10^{11}$
6	4	$0.102\,253\,200\,000\,0000\times10^{8}$	6	5	$-0.121\,195\,200\,000\,0000\times10^{8}$	13	1	$-0.927\,546\,307\,609\,0287\times10^{14}$	13	2	$0.269\,197\,943\,895\,8787\times10^{15}$
6	6	$0.409\,516\,800\,000\,0000\times10^{7}$	7	1	$0.177\,694\,040\,000\,0000\times10^{8}$	13	3	$-0.262\,750\,156\,396\,8941\times10^{15}$	13	4	$0.795\,305\,043\,317\,2421\times10^{14}$
7	2	$-0.134\,576\,740\,000\,0000\times10^{8}$	7	3	$-0.329\,945\,800\,000\,0000\times10^{8}$	13	5	$0.111\,029\,292\,748\,8947\times10^{14}$	13	6	$0.269\,025\,146\,403\,5798\times10^{13}$
7	4	$0.463\,702\,400\,000\,0000\times10^{7}$	7	5	$0.762\,350\,400\,000\,0000\times10^{8}$	13	7	$-0.100\,352\,792\,939\,7055\times10^{14}$	13	8	$0.372\,139\,000\,129\,6261\times10^{13}$
7	6	$-0.724\,711\,680\,000\,0000\times10^{8}$	7	7	$0.203\,554\,560\,000\,0000\times10^{8}$	13	9	$-0.475\,969\,657\,610\,9528\times10^{12}$	13	10	$-0.989\,777\,389\,568\,0000\times10^{12}$
8	1	$0.248\,507\,370\,807\,8464\times10^{8}$	8	2	$0.157\,580\,193\,865\,4665\times10^{9}$	13	11	$0.117\,477\,590\,630\,4000\times10^{13}$	13	12	$-0.480\,865\,222\,656\,0000\times10^{12}$
8	3	$-0.152\,823\,389\,198\,5847\times10^{9}$	8	4	$-0.191\,777\,555\,747\,6664\times10^{9}$	13	13	$0.688\,847\,093\,760\,0000\times10^{11}$	14	1	$-0.915\,866\,802\,231\,9353\times10^{15}$
8	5	$-0.328\,513\,920\,000\,0000\times10^{8}$	8	6	$0.485\,102\,688\,000\,0000\times10^{9}$	14	2	$0.120\,059\,707\,299\,7821\times10^{16}$	14	3	$0.829\,182\,442\,249\,7396\times10^{15}$
8	7	$-0.381\,988\,992\,000\,0000\times10^{9}$	8	8	$0.920\,325\,120\,000\,0000\times10^{8}$	14	4	$-0.194\,839433\,126\,8593\times10^{16}$	14	5	$0.946\,131\,686\,858\,9581\times10^{15}$
9	1	$-0.313\,446\,076\,716\,9980\times10^{10}$	9	2	$0.655\,359\,213\,235\,5817\times10^{10}$	14	6	$-0.108\,510\,806\,913\,9926\times10^{15}$	14	7	$0.297\,586\,678\,672\,8232\times10^{14}$
9	3	$-0.326\,496\,820\,439\,7003\times10^{10}$	9	4	$0.215\,873\,652\,393\,3126\times10^{9}$	14	8	$-0.475\,726\,461\,594\,4131\times10^{14}$	14	9	$0.176\,807\,640\,207\,2156\times10^{14}$
9	5	$-0.107\,450\,705\,518\,2147\times10^{10}$	9	6	$-0.584\,308\,032\,000\,0000\times10^{9}$	14	10	$-0.150\,963\,049\,976\,6138\times10^{13}$	14	11	$-0.461\,975\,241\,728\,0000\times10^{13}$
9	7	$0.272\,708\,620\,800\,0000\times10^{10}$	9	8	$-0.182\,351\,769\,600\,0000\times10^{10}$	14	12	$0.461\,203\,734\,118\,4000\times10^{13}$	14	13	$-0.171\,671\,317\,708\,8000\times10^{13}$
9	9	$0.385\,409\,024\,000\,0000\times10^{9}$	10	1	$-0.443\,351\,897\,286\,5159\times10^{10}$	14	14	$0.228\,012\,490\,752\,0000\times10^{12}$	15	1	$0.208\,118\,176\,945\,6836\times10^{17}$
10	2	$-0.313\,595\,395\,048\,2084\times10^{11}$	10	3	$0.764\,264\,858\,187\,8701\times10^{11}$	15	2	$-0.690\,031\,916\,769\,5184\times10^{17}$	15	3	$0.836\,819\,775\,557\,3149\times10^{17}$
10	4	$-0.479\,252\,551\,930\,0435\times10^{11}$	10	5	$0.108\,267\,054\,086\,3647\times10^{11}$	15	4	$-0.417\,288\,028\,393\,9998\times10^{17}$	15	5	$0.332\,203\,240\,822\,9609\times10^{16}$
10	6	$-0.577\,958\,588\,273\,3134\times10^{10}$	10	7	$-0.511\,015\,680\,000\,0000\times10^{10}$	15	6	$0.381\,406\,365\,810\,5405\times10^{16}$	15	7	$-0.979\,995\,583\,459\,4928\times10^{15}$
10	8	$0.138\,753\,457\,920\,0000\times10^{11}$	10	9	$-0.803\,516\,313\,600\,0000\times10^{10}$	15	8	$0.229\,254\,567\,554\,8962\times10^{15}$	15	9	$-0.211\,582\,019\,271\,2246\times10^{15}$
10	10	$0.151\,498\,547\,200\,0000\times10^{10}$	11	1	$0.471\,994\,382\,248\,5929\times10^{12}$	15	10	$0.758\,805\,741\,406\,4968\times10^{14}$	15	11	$-0.348\,216\,242\,380\,9559\times10^{13}$
11	2	$-0.110\,656\,123\,435\,3233\times10^{13}$	11	3	$0.619\,766\,094\,233\,7001\times10^{12}$	15	12	$-0.201\,254\,479\,462\,4000\times10^{14}$	15	13	$0.173\,335\,792\,680\,9600\times10^{14}$
11	4	$0.282\,005\,688\,446\,9608\times10^{12}$	11	5	$-0.345\,651\,944\,276\,4311\times10^{12}$	15	14	$-0.591\,270\,268\,108\,8000\times10^{13}$	15	15	$0.732\,396\,060\,672\,0000\times10^{12}$

algorithms as different as these, strongly indicates that both must be correct. Since our method is highly computerized, this suggests that our other elements must also be reliable. Checks have been made on the elements up to 13th order by calculations from the complete graph lists as well as from the NFE ones.

III. ANALYSIS

A. Methods

We have analyzed the series presented above as well as some of the series from Ref. 23. We have analyzed the individual series presented above, with two different methods,[11,12,45–48] based on the assumption that there are nonanalytic confluent corrections to scaling and one[49] based on the assumption that there are logarithmic confluent corrections. Each calculation that was made for the individual series was threshold biased, but since a very large range of trial thresholds was selected all possible values were allowed for. In addition to the analyses of the individual series, we have studied various combinations of the series for the different moments and of the series obtained by squaring individual moments. These combinations[13,50] eliminate the need for prior knowledge of the exact percolation threshold. They are therefore an important tool for the percolation problem where threshold uncertainty has really interfered with past analyses.

It should be noted that many of the analyses that were not threshold biased were made by the following "blind" procedure. First we assigned each series a different identifying number and then analyzed them in random order, without regard to identity. The results were then identified and tabulated. This procedure ensured that no prior bias from the "expected" results interfered with the determination of the critical exponents. We believe that this is an important precaution when analyzing series for problems about which considerable information is available.

Our approach to the analyses of a set of series for a sequence of moments and for an arbitrary set of dimensions has been discussed at length in many of our earlier papers.[5,13,33,34,38] The series presented in the previous section are similar to those in these references where both the strengths and potential pitfalls of our analysis are presented. Work with test series and exactly solved models has demonstrated that our combination of methods gives at least a three-significant-figure reliability for dominant exponent estimates in models for which 15-term low-density series alone are available. Improved accuracy is found when high-density series are also available[48] as is the case for percolation in three dimensions. Further work on test series will be presented in Ref. 38.

The analyses based on the assumption of nonanalytic confluent corrections to scaling assume that the series being studied, denoted by $H(p)$ in general, has the form

$$H(p)=A(p_c-p)^{-h}[1+a(p_c-p)^{\Delta_1}+b(p_c-p)+\ldots], \tag{3.1}$$

where h is the critical exponent that we wish to determine. In the first method of analysis, denoted below as $M1$,[47] we study the logarithmic derivative of

$$B(p)=hH(p)-(p_c-p)\left[\frac{dH(p)}{dp}\right], \tag{3.2}$$

which has a pole at p_c with residue $-h+\Delta_1$. For a given value of p_c we obtain graphs of Δ_1 versus input h for all Padé approximants, and we choose the triplet p_c,h,Δ_1 where all Padés converge to the same point. In the second method, denoted below as $M2$,[12,47] we first transform the series in p into a series in the variable y, where

$$y=1-(1-p/p_c)^{\Delta_1},$$

and then take Padé approximants to

$$G(y)=\Delta_1(y-1)\frac{d}{dy}\ln(H(p)), \tag{3.3}$$

which should converge to $-h$. Here we plot graphs of h versus the input Δ_1 for different values of p_c and choose again the triplet p_c,h,Δ_1, where all Padés converge to the same point. When $\Delta_1=1.0$ this method reduces[12] to the usual biased d log Pade method. We carried out preliminary unbiased d log Padé analyses of the $S(p)$ series to obtain approximate initial estimates of γ and p_c. These estimates are close to the values seen at $\Delta_1=1.0$ in the $M2$ method, making them reasonable only in those cases where the true Δ_1 is near unity. Both of those methods have proven very useful for many problems, but do require the simultaneous determination of three critical quantities.

In addition to the above temperature-biased analyses of individual series we have also used an old method[50] (see also Ref. 13), involving term-by-term dividing two series with the same critical threshold and then studying the "divided" series. If we begin with two series expansions $Y=\sum_{j=0,n}y_jp^j$ and $Z=\sum_{j=0,n}z_jp^j$ then we shall denote the term-by-term divided series, $\sum_{j=0,n}(y_j/z_j)p^j$, by $Y\div Z$. This divided series should have critical behavior with a threshold at $p=1$ and a dominant critical exponent equal to the difference between the exponents of the two original series plus 1. The division is expected to introduce an analytic correction to scaling (i.e., $\Delta_1=1$). If this correction has a large enough amplitude it could provide a nice convergence region for the evaluation of the dominant exponent. It is to be hoped that the amplitude of the introduced analytic correction is sufficient to swamp the nonanalytic correction of the individual series which is still present. This method avoids the problems associated with uncertainties in p_c, but convergence is poorer owing to competing effects of the two corrections.

One possible way to obtain exponents from a single series $H(p)$ when we are uncertain of the exact threshold is to utilize the above approach with series Y being $(H(p))^2$, and series Z being $H(p)$ itself. We call the resultant series, which has a critical exponent of $h+1$, a "self-divided" series, and denote it by H^{sd}.

We note that for both the term-by-term divided series and temperature-biased series, it is important to use both $M1$ and $M2$ for each case. This is because for certain tests[38,47] and well-behaved model[48] series the $M2$ analysis

gives the correct dominant exponent estimate with intersection regions at the correct Δ_1 and also at resonance Δ_1/n values. Thus, it would be difficult to identify the correct Δ_1 value if we did not also have the $M1$ method which is resonance free.[38] We do not use $M1$ alone as test series work suggests that it gives Δ_1 estimates which are less accurate than the $M2$ ones when Δ_1 is far from an integer. The use of two methods also eliminates the possibility that accidental spurious convergence regions will be confused with the correct results. Attention should be payed to the fact that in $M1$ we input h, whereas in $M2$ we input Δ_1. This means that the $M1$ graphs may have multiple values of h for a single Δ_1 choice, whereas in $M2$ the opposite is true. We have chosen to present both analyses with the same axes for ease of comparison.

The assumption of logarithmic corrections entails fitting to the form

$$H(p)=(p_c-p)^{-h}|\ln(p_c-p)|^{\theta} . \tag{3.4}$$

We fitted this form with the method of Adler and Privman.[49] The analysis of the logarithmic form involves writing $\theta=zh$ and then taking Padé approximants to the series

$$g(p)=(-h)^{-1}(p_c-p)\ln(p_c-p) \times\{[H(p)'/H(p)]-[h/(p_c-p)]\} . \tag{3.5}$$

We can show that the limit of $g(p)$ as $p\to p_c$ is z. We take Padé approximants to g at the exact or most reliable estimate of p_c to obtain graphs of θ as a function of h.

B. Above the upper critical dimension

In our previous study[33] of the high-dimensional percolation series we gave estimates for the thresholds in $7\le d\le 9$ from the 11th-order series. These are quoted in Table II, and we note that they are based on the mean cluster size ($j=2$) alone since we did not reexamine $d>6$ in Ref. 5. We saw corrections to scaling at $\Delta_1=0.5$ and 1.0 in $d=7$ and 8, in agreement with $\Delta_1=(d-6)/2$ that came from the exact result near the Gaussian fixed point.[33] However, in $d=8$ we also saw a resonance at $\Delta_1=\frac{1}{2}$.

In the analysis of the 15th-order series we found the thresholds at $d=8$ and 9 to be unchanged from Ref. 33 when we studied the mean cluster size and some of the higher moments. The best convergence in the longer series was very close to that of the shorter series and we see no reason to change the central values of the error ranges. It would be quite reasonable to reduce the size of the error bounds based on the quality of the convergence, but we prefer not to in case we have neglected any systematic errors. For $d=8$ and 9 we again saw analytic corrections.

At $d=7$ we could see a clear convergence to a value of $\Delta_1=0.35$, slightly below the predicted result of $\Delta_1=0.5$ for a threshold of $p_c=0.078\,685$ slightly above that cited[33] by us ($p_c=0.078\,62\pm0.000\,03$) and closer to the older values. This was the best convergence seen for this dimension and was superior to that at $p_c=0.078\,62$. At the old value exponents $\Delta_1=1.0$ and $\gamma=1.0$ are seen. For $p_c=0.078\,680$ exponents of $\Delta_1=0.5$ and $\gamma=1.0$ are seen, but the convergence is a little weaker than at the higher value.

C. Six dimensions

At six dimensions the correct behavior[3,4] is given by Eq. (1.3) for $S(p)$ (which is equivalent to Γ_2) and by Eq. (3.4) with $\theta=\frac{2}{7}$ and $\gamma_j=2j-1$ for Γ_j. From a study of the $S(p)$, $S(p)'$, and Γ_3 series we found the best convergence to these values for $p_c=0.0942$. We found that op-

TABLE IV. Our estimates for h and Δ_1 from the divided series.

			($\Delta_1=1.0$)		(Best convergence)			
d	Series	h	$h(M1)$	$h(M2)$	$h(M1)$	$\Delta_1(M1)$	$h(M2)$	$\Delta_1(M2)$
3	sc $S(p)^{sd}$	γ	1.82	1.81	1.83	1.0	1.90	0.8
3	sc $(S_{sb})^{sd}$	γ	1.90	1.82	1.80	1.1	1.85	0.9
3	sc $(S_{bb})^{sd}$	γ				>1.5	1.72	1.25
3	bcc $(S_{ss})^{sd}$	γ	1.85	1.85	1.83	1.05	1.90	0.8
3	bcc $(S_{sb})^{sd}$	γ	1.90	1.86	1.75	1.3	1.80	1.2
3	bcc $(S_{bb})^{sd}$	γ		1.70		>1.5	1.72	1.2
3	sc Γ_3^{sd}	$2\gamma+\beta$	4.2	4.0		>1.5	3.9	1.3
3	sc Γ_4^{sd}	$3\gamma+2\beta$	6.2	6.2		>1.5		>1.5
3	sc $\Gamma_3\div S(p)$	Δ	2.20	2.14				
3	sc $\Gamma_4\div\Gamma_3$	Δ	2.20	2.18				
4	hc $S(p)^{sd}$	γ	1.39	1.37	1.44	0.8	1.41	0.8
4	hc Γ_3^{sd}	$2\gamma+\beta$	3.45	3.45	3.70	0.5	3.45	1.0
4	hc Γ_4^{sd}	$3\gamma+2\beta$			5.45	1.75	5.4	1.8
4	hc $\Gamma_3\div S(p)$	Δ	2.08	2.08	2.06	1.3	2.07	1.1
4	hc $\Gamma_4\div\Gamma_3$	Δ	2.07	2.08	2.07	1.0	2.08	1.0
5	hc $S(p)^{sd}$	γ	1.18	1.18	1.18	0.5	1.18	0.6
5	hc Γ_3^{sd}	$2\gamma+\beta$	3.20	3.20	3.25	0.7	3.23	0.8
5	hc Γ_4^{sd}	$3\gamma+2\beta$			5.25	0.7	5.10	1.3
5	hc $\Gamma_3\div S(p)$	Δ	2.025	2.025	2.025	1.0	2.015	1.2
5	hc $\Gamma_4\div\Gamma_3$	Δ	2.025	2.017			2.015	1.1

timal convergence occurred near these values. This p_c estimate is again a little above the value from the 11-term series.[33]

D. Below the upper critical dimension

In dimensions $d=3-5$ we are interested in obtaining the critical exponents and thresholds to the highest precision possible. Our strategy has been as follows: For each lattice we begin by studying the various possible term-by-term divided series in order to remove any possibility of threshold bias. Series studied included Γ_j^{sd} and various combinations of $\Gamma_j \div \Gamma_k$ with $k<j$. Results for $d=3-5$ are given in Table IV. Using these exponent estimates and the criteria of convergence of Padé plots, we have then selected thresholds for each lattice from a study of the $S(p)$ series for different trial thresholds. We have revised the exponent estimates if the convergence was outstanding relative to that of the divided series. We have then studied the higher moments near the central threshold in order to obtain improved β estimates. (In the event that clear convergence would be seen here, we would again revise thresholds self-consistently if needed, but such a scenario did not eventuate with these series.) The threshold biased exponent values are presented in Table V, for those thresholds sufficiently near convergence to merit consideration as serious contenders. There is an error of $\pm\frac{1}{2}$ of the last quoted digit in each table entry from the limit of reading error from the graphs. The errors from poor convergence are taken into account in the conclusions from the table. We have reported results both for optimal correction exponent convergence and at value of an analytic correction, $\Delta_1=1.0$. Results in the columns of $\Delta_1=1.0$ are absent in the cases where no results corresponded to this correction. We present both cases in order that the corresponding d log

TABLE V. Our estimates for h and Δ_1 from the temperature-biased series.

				($\Delta_1=1.0$)		(Best convergence)			
d	Series	Threshold	h	$h(M1)$	$h(M2)$	$h(M1)$	$\Delta_1(M1)$	$h(M2)$	$\Delta_1(M2)$
3	sc $S(p)$	0.2492	γ	1.85	1.85	1.86	0.9	1.86	0.95
3	sc $S(p)$	0.2490	γ	1.83	1.82	1.83	1.0	1.83	0.95
3	sc $S(p)$	0.2488	γ	1.81	1.81	1.81	1.1	1.80	1.05
3	sc $S(p)$	0.2486	γ	1.79	1.79	1.79	1.1	1.79	1.05
3	sc Γ_3	0.2492	$2\gamma+\beta$	4.025	4.1				
3	sc Γ_3	0.2488	$2\gamma+\beta$	4.01	4.01	4.02	0.8	4.02	1.45
3	sc Γ_3	0.2486	$2\gamma+\beta$	4.0	4.0				
3	sc Γ_4	0.2488	$3\gamma+2\beta$	6.23		6.24	1.15	6.26	1.5
3	bcc S_{ss}	0.180 75	γ	1.87		1.9	0.80	1.91	0.7
3	bcc S_{ss}	0.180 50	γ	1.83	1.83	1.84	0.95	1.85	0.95
3	bcc S_{ss}	0.180 30	γ	1.815	1.82	1.815	1.0	1.82	1.2
3	bcc S_{ss}	0.180 20	γ	1.81	1.80	1.795	1.3	1.80	1.2
3	bcc S_{ss}	0.179 50	γ	1.76		1.75	1.2	1.78	1.3
3	sc $P(p)$	0.2494	β		0.42	0.38	1.3	0.385	1.1
3	sc $P(p)$	0.2489	β		0.43	0.40	1.2	0.400	1.1
3	sc $P(p)$	0.2488	β		0.43	0.405	1.2	0.405	1.1
3	sc $P(p)$	0.2487	β		0.43	0.41	1.2	0.405	1.1
3	sc $P(p)$	0.2486	β		0.43	0.41	1.15	0.410	1.1
3	bcc $P(p)$	0.1803	β	0.43	0.425	0.405	1.1	0.41	1.1
3	bcc $P(p)$	0.1802	β	0.43	0.430	0.405	1.1	0.41	1.1
4	hc $S(p)$	0.160 200	γ						
4	hc $S(p)$	0.160 100	γ		1.43	1.44	0.6	1.44	0.6
4	hc $S(p)$	0.160 075	γ		1.42	1.425	0.7	1.44	0.6
4	hc $S(p)$	0.160 050	γ		1.415	1.425	0.7	1.435	0.6
4	hc $S(p)$	0.160 025	γ		1.41	1.42	0.7	1.425	0.7
4	hc $S(p)$	0.160 000	γ		1.405	1.415	0.7	1.42	0.7
4	hc $S(p)$	0.159 900	γ		1.38	1.39	0.8	1.39	0.8
4	hc Γ_3	0.1602	$2\gamma+\beta$	3.5	3.5	3.5	0.8	3.5	1.0
4	hc Γ_3	0.1601	$2\gamma+\beta$	3.49	3.51			3.50	1.1
4	hc Γ_3	0.1600	$2\gamma+\beta$	3.48	3.49			3.485	1.1
4	hc Γ_3	0.1599	$2\gamma+\beta$	3.47	3.47			3.475	1.5
4	hc Γ_4	0.1600	$3\gamma+2\beta$		5.56	5.56	1.1	5.58	1.4
5	hc $S(p)$	0.118 23	γ			1.20	0.4		
5	hc $S(p)$	0.118 20	γ			1.19	0.5	1.19	0.5
5	hc $S(p)$	0.118 19	γ			1.185	0.6	1.185	0.5
5	hc $S(p)$	0.118 18	γ			1.18	0.65	1.18	0.6
5	hc $S(p)$	0.118 17	γ					1.18	0.8
5	hc Γ_3	0.118 19	$2\gamma+\beta$	3.2025	3.2025	3.2025		3.2025	1.0
5	hc Γ_4	0.118 19	$3\gamma+2\beta$	5.225	5.225	5.23	1.05	5.235	1.1

Padé value can easily be read off for $M2$, and in order to give an idea of the difference in the two cases. Unless specifically stated, we do not observe convergence at $\Delta_1=1.0$. We have also calculated ν and η values from our β and γ estimates via the hyperscaling and scaling relations $d\nu=2-\alpha=2\beta+\gamma$, and $\gamma=\nu(2-\eta)$. These have been entered into Table I.

In five dimensions we observed excellent convergence. The divided series give $\Delta=2.02$ and if we combine this with the $\gamma=1.18$ that comes from the self-divided $S(p)$ series then we have $\beta=0.84$. These values are also in good agreement with the self-divided higher moments. The $\gamma=1.18$ choice corresponds to a threshold of 0.118 18, although convergence is marginally better at 0.118 19. Using the $\gamma=1.185$ seen at $p_c=0.118\,19$ and the Γ_3 exponent at this threshold we obtain $\beta=0.8325$, while from the Γ_4 exponent we deduce $\beta=0.8375$. This gives overall estimates of $p_c=0.118\,19\pm0.000\,04$, $\gamma=1.185\pm0.005$, $\beta=0.835\pm0.005$, and $\Delta=2.02\pm0.01$. The exponent γ is a little lower than that seen from the 11-term series, the central threshold is similar. We find $\nu=0.571\pm0.003$ and $\eta=-0.075\pm0.020$ from scaling. We present some graphs of Padé approximants to γ and $3\gamma+2\beta$ in Fig. 2. We measure $\Delta_1=0.55\pm0.15$ from the threshold-biased series.

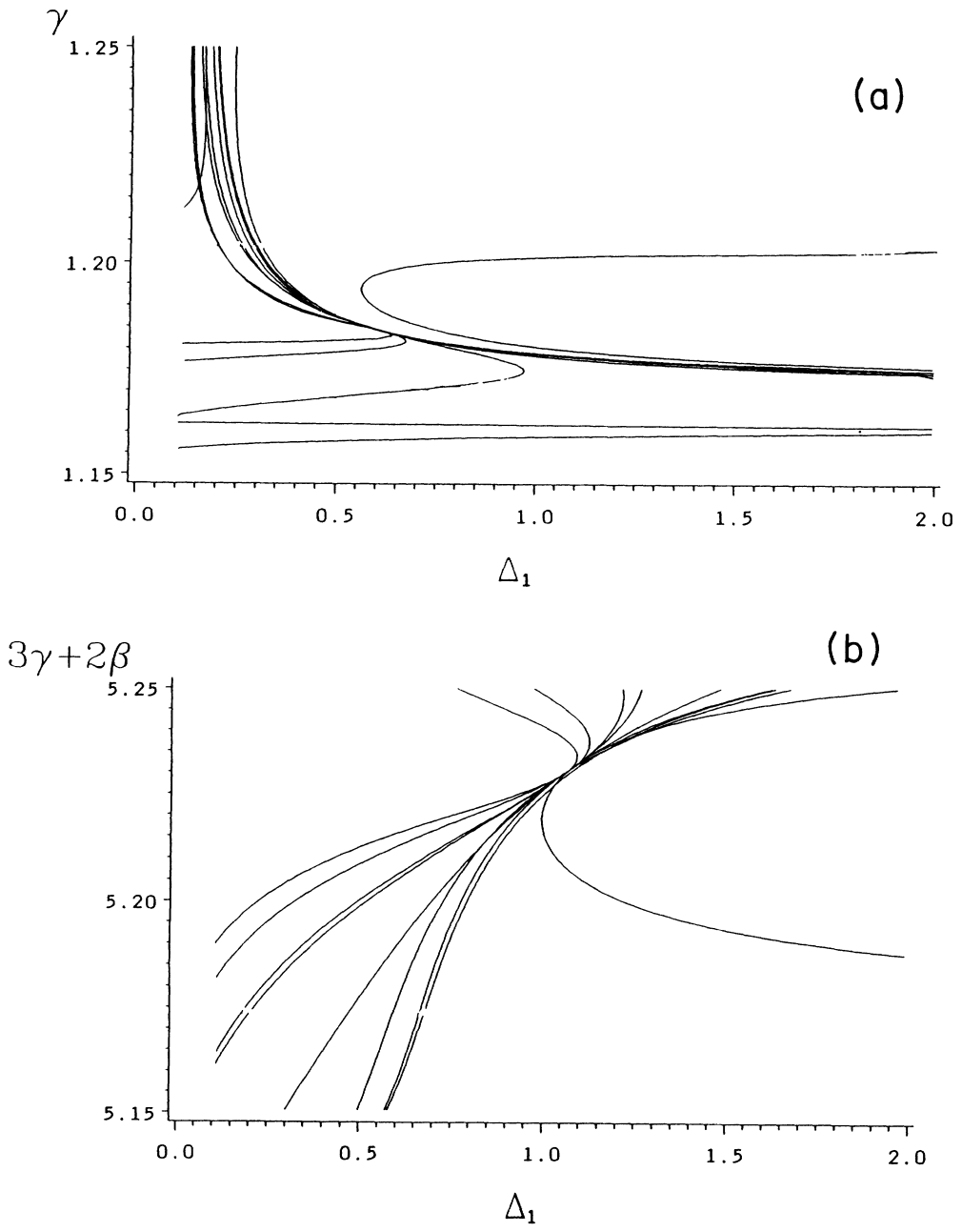

FIG. 2. Graphs of selected central and near-diagonal Padé approximants to (a) γ as a function of Δ_1 from the $M1$ analysis of $S(p)$ at $p_c=0.118\,19$, (b) $3\gamma+2\beta$ as a function of Δ_1 from the $M1$ analysis of Γ_4 at $p_c=0.118\,19$ for the five-dimensional series.

In four dimensions we have a small inconsistency between the different methods of analysis for the Γ_4 series, but we are still able to make accurate exponent estimates. The $S(p)^{sd}$ series gives $\gamma=1.42$. This value corresponds to a threshold of 0.160 000 or 0.160 025. For the threshold-biased $S(p)$ series we see superior convergence near $p_c=0.1601$ (which corresponds to $\gamma\approx 1.44$). Both these values are below those of the 11-term series, where optimal convergence was seen at our old p_c choice of 0.1603. For both series we have roughly the same behavior of γ as a function of p_c and Δ_1, but as the length increases optimal convergence moves a little down in p_c, and therefore to slightly lower γ values. The Γ_3^{sd} series analyses give an average exponent of $2\gamma+\beta=3.51$ which corresponds to $p_c=0.1601$. Here convergence was better at 0.1600. Thus, we choose as the central p_c value 0.160 05, and give $p_c=0.160\,05\pm0.000\,15$ with $\gamma=1.435\pm0.015$. The measurements of Δ from the divided series average out to 2.074 ± 0.006, which gives a β estimate of 0.639 ± 0.02. These results give $3\gamma+2\beta=5.583\pm0.12$ which is consistent with the directly measured γ_4 value, but higher than that from the Γ_4^{sd} series. The convergence of the latter was poor, but that of the threshold-biased series was quite reasonable for the range

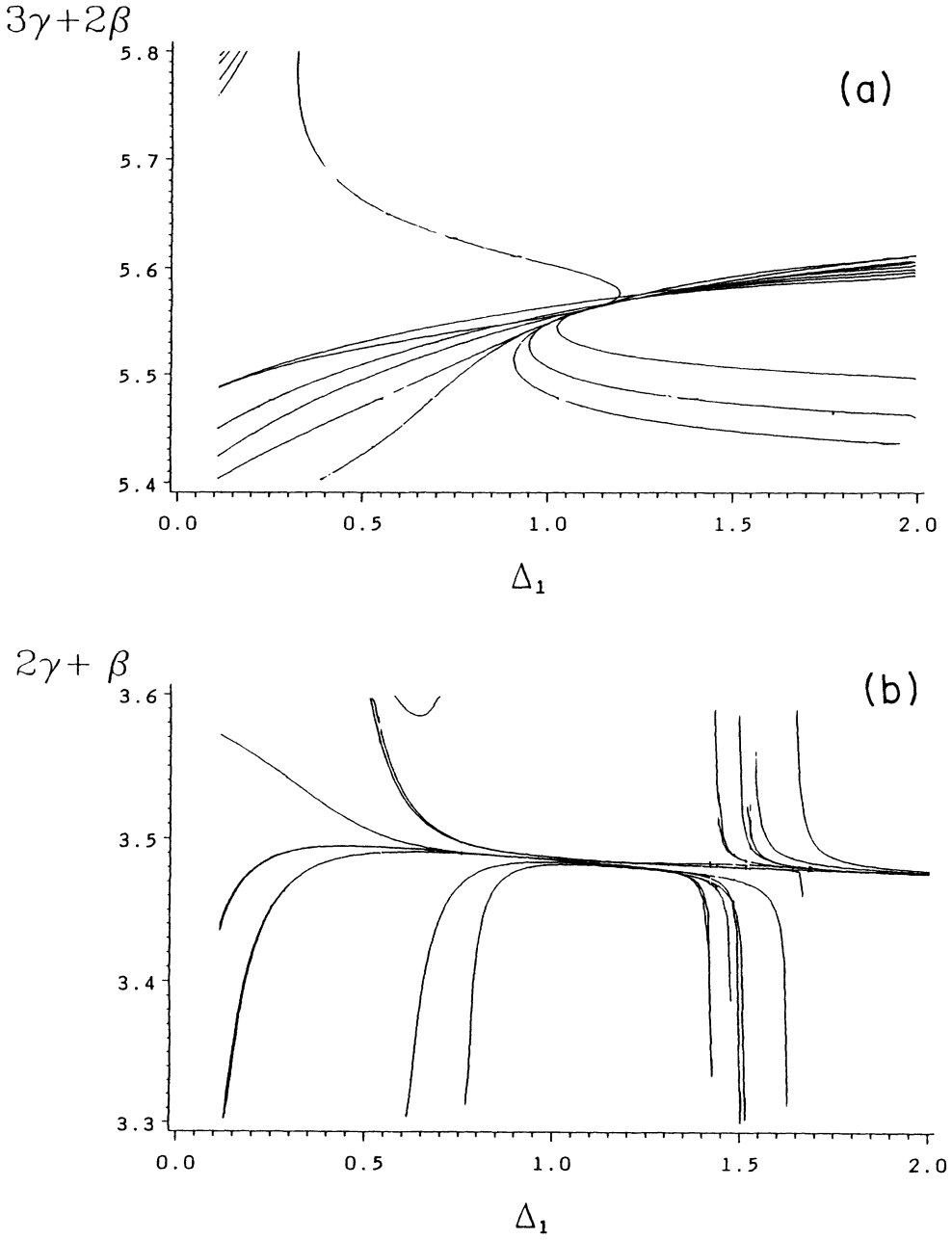

FIG. 3. Graphs of selected central and near-diagonal Padé approximants to (a) $3\gamma+2\beta$ as a function of Δ_1 from the $M1$ analysis of Γ_4 at $p_c=0.1600$, (b) $2\gamma+\beta$ as a function of Δ_1 from the $M2$ analysis of Γ_3 at $p_c=0.1600$ for the four- dimensional series.

of thresholds that corresponded to that where good convergence was found for $S(p)$. We present a graph of Padé approximants to $3\gamma+2\beta$ at $p_c=0.1600$ in Fig. 3(a) and a graph of Padé approximants to $2\gamma+\beta$ at $p_c=0.1600$ in Fig. 3(b). Note that both these series appear to have an analytic correction only, but in the $S(p)$ series we see $\Delta_1=0.65\pm0.10$. We presume that in the case of the higher moments the amplitude of the nonanalytic correction to scaling term is very small. The four-dimensional exponent estimates lead, via scaling, to $\nu=0.678\pm0.050$ and $\eta=-0.12\pm0.05$.

For three dimensions we have undertaken an analysis of the 14-term bcc and simple cubic- (sc) bond-percolation series of Sykes and Wilkinson[23] for three alternate definitions of the mean cluster size in addition to our new series. The results from both sets of series are

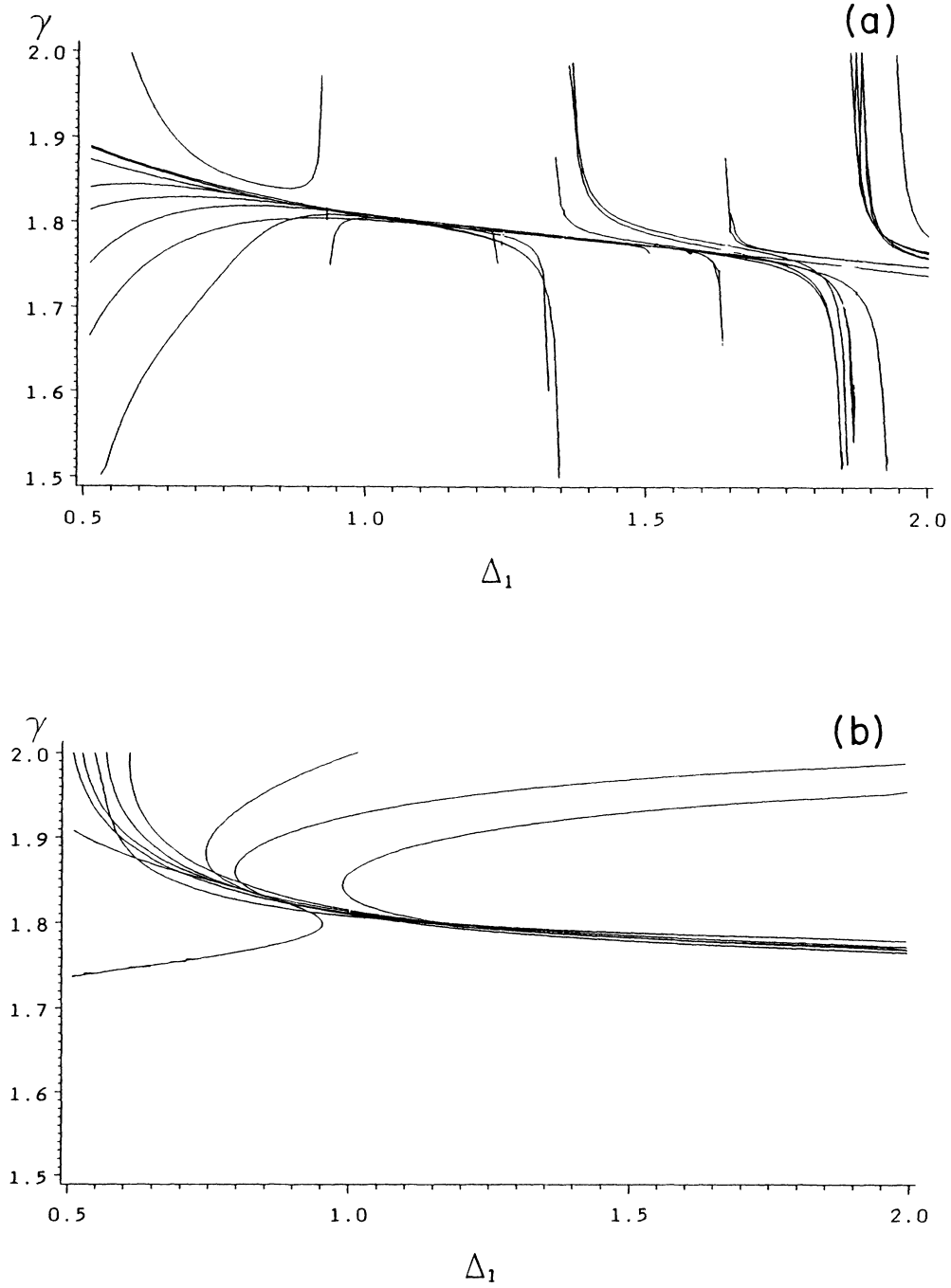

FIG. 4. Graphs of selected central and near-diagonal Padé approximants to (a) γ as a function of Δ_1 from the $M2$ analysis of $S(p)$ at $p_c=0.2488$ for the sc lattice, (b) γ as a function of Δ_1 from the $M1$ analysis of $S(p)$ at $p_c=0.2488$ for th sc lattice, (c) γ as a function of Δ_1 from the $M2$ analysis of $S(p)$ at $p_c=0.1802$, (d) γ as a function of Δ_1 from the $M1$ analysis of $S(p)$ at $p_c=0.1803$ for the bcc lattice for the three-dimensional low-density series.

given in Tables IV and V. We use their notation to distinguish between their different series, and note that the first 14 terms of our $S(p)$ series are identical to their *ss* (mean size of clusters with s sites connected to an occupied site) series for the simple-cubic lattice. Although these series are one term shorter, we expect good results from the bcc calculation since this lattice is closer packed than the sc.

From the various 3D estimates for γ from the term-by-term low-density divided series we find an average value of $\gamma=1.83$. For the best converged results we obtain an average of $\gamma=1.82$. For the sc $S(p)$ series we find the best convergence around $p_c=0.2488$ from $M1$ and a little lower from $M2$. Convergence definitely deteriorates above $p_c=0.2491$ and excludes the old[24] estimates of 0.2492 and 0.2494. At $p_c=0.2488$ we find $\gamma=1.805$, which is a little lower than that seen in the divided series. For the bcc series we find optimal convergence around $p_c=0.1802$ for $M2$ and $p_c=0.1803$ for $M1$. An averaged estimate at these thresholds gives $\gamma=1.81$. We present graphs of different Padé approximants to γ as a function of Δ_1 for the best converged series in Fig. 4. We propose the overall values of $p_c(\text{sc})=0.2488\pm0.0002$ and $p_c(\text{bcc})=0.180\,25\pm0.000\,15$. These give $\gamma=1.81\pm0.02$ and $\gamma=1.805$ at the optimal sc convergence. The threshold-biased results are consistent with a correction exponent of $\Delta_1=1.1\pm0.2$.

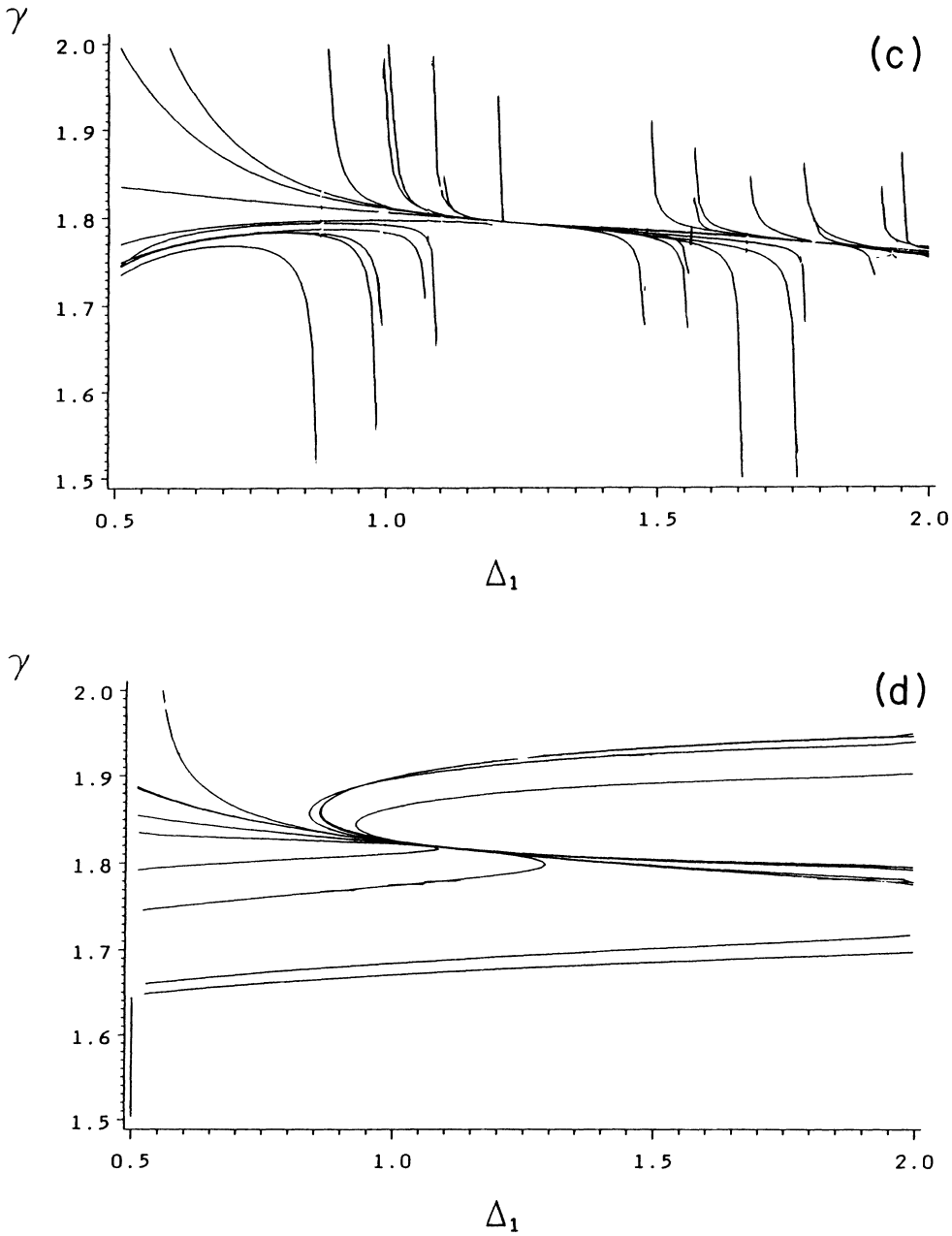

FIG. 4. (*Continued*).

For the other exponents we find $\Delta=2.18\pm0.02$ from the divisions of the successive moments and if we use the above $\gamma=1.81(1.805)$ estimates we find $\beta=0.37(0.375)$. If we use the self-divided series we find $2\gamma+\beta=4.0\pm0.1$ and $3\gamma+2\beta=6.2$. Optimal convergence in the Γ_3 series gives $2\gamma+\beta=4.01$. We note that for the Γ_3 series the graph of $2\gamma+\beta$ as a function of Δ_1 is extremely flat. The best convergence for Γ_4 gives $3\gamma+2\beta=6.25$. Using $\gamma=1.81(1.805)$ this leads us to estimates of $\beta=0.38(0.39)$, $0.385(0.392)$, $0.39(0.40)$, and $0.41(0.42)$. We suggest the overall estimate $\beta=0.40\pm0.02$ from the low-density series. This value is below the older series and simulation results but still substantially above the central field theoretic estimates.[16,30]

We have also considered the high-density series[23] for $P(p)$ and $S(p)$. The $S(p)$ series did not converge very well for $M2$ and $M1$ results were broadly consistent with the low-density values. We did not do any analyses of divided series because of the large number of zero terms. The $P(p)$ series converged very nicely indeed. In contrast to the low-density results for γ which are strongly dependent on the p_c choice and far less so on Δ_1, these series are only weakly dependent on p_c but very strongly dependent (percentagewise) on Δ_1. A typical graph of β as a function of Δ_1 for the 61-term sc bond series at $p_c=0.2488$ is given in Fig. 5(a). Optimal convergence is at $\beta=0.405$ (with $\Delta_1=1.1$ in close agreement with the low-density result), but if we use the idea of a box sur-

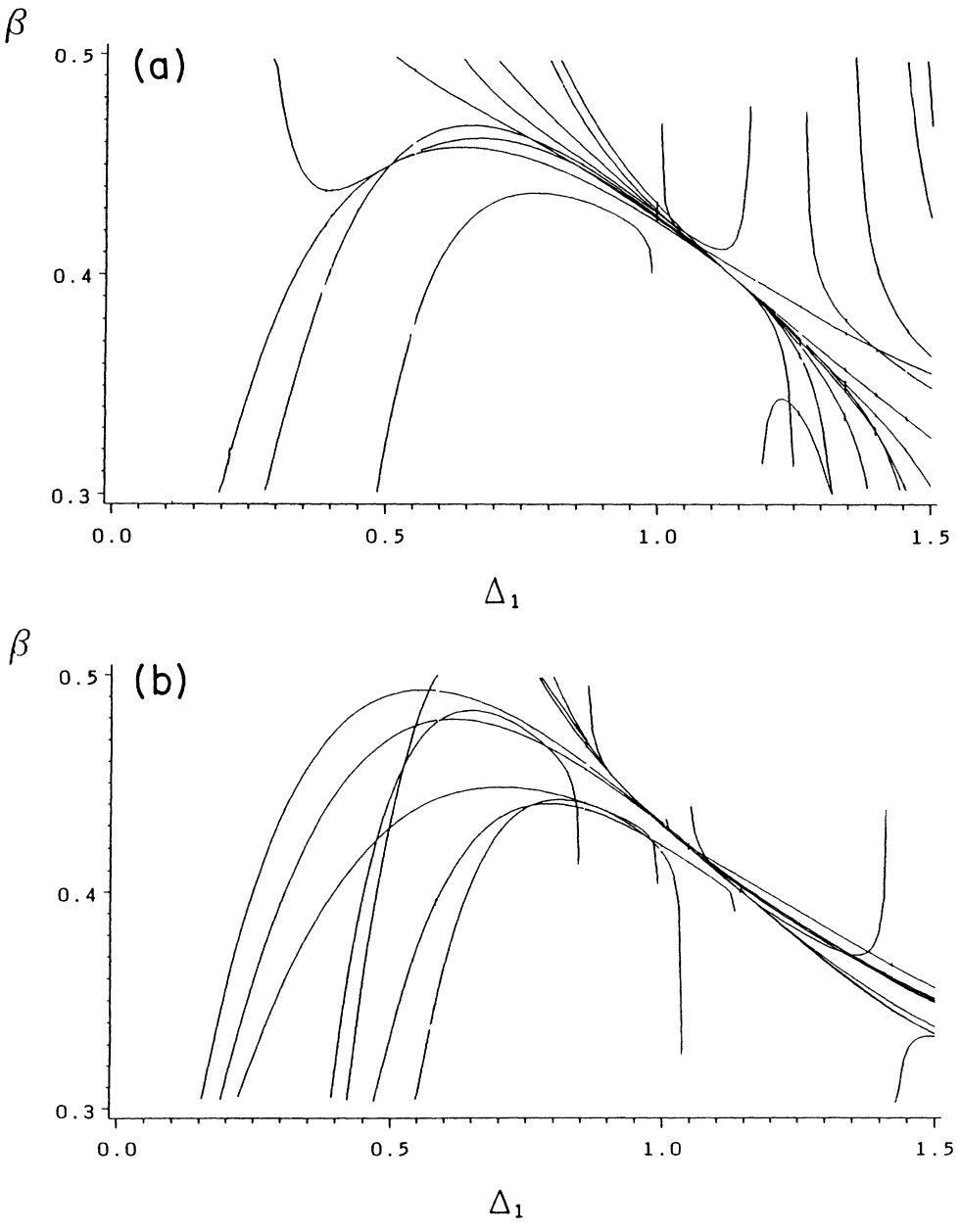

FIG. 5. Graphs of selected central and near-diagonal Padé approximants to (a) β as a function of Δ_1 from the $M2$ analysis of $P(p)$ at $p_c=0.2488$, (b) β as a function of Δ_1 from the $M2$ analysis of $P(p)$ at $p_c=0.1803$ for the three-dimensional high-density series.

rounding the region of convergence we see that the range 0.385 to 0.415 must be included for β. Similar behavior is seen for the 41-term bcc series, illustrated in Fig. 5(b). These values suggest that we should revise our β estimate slightly upwards and imply that the β estimate from the temperature-biased Γ_3 and Γ_4 series may be more accurate than those from the divided series. We suggest an overall $\beta=0.405\pm0.025$. Together with the preferred $\gamma=1.805\pm0.02$ we have $\Delta=2.21\pm0.04$. This gives us $\nu=0.872\pm0.070$ and $\eta=-0.07\pm0.05$.

IV. AMPLITUDE RATIOS

In addition to the critical exponents, certain amplitude ratios are also universal quantities. These may also serve to characterize the universality class. This is especially relevant to the percolation problem due to the recent claim of differing amplitude ratios for lattice and continuum percolation.[17] Thus, accurate estimates of the amplitude ratios are desirable. We used a method introduced in Ref. 13 to estimate the related universal quantities

$$S_{ij/kl}=(A_i A_j/A_k A_l)K_{ij/kl} ,$$

where

$$K_{ij/kl}=\frac{\Gamma(\gamma_k)\Gamma(\gamma_l)}{\Gamma(\gamma_i)\Gamma(\gamma_j)} ,$$

and Γ is the usual γ function. The A_i are defined in Eq. (1.4). In this method we analyze the series $\sum_n c_n^{ij/kl}p^n$, where,

$$c_n^{ij/kl}\equiv a_n^{(i)}a_n^{(j)}/a_n^{(k)}a_n^{(l)} , \tag{4.1}$$

and $a_n^{(l)}$ is the coefficient of p^n in the series for Γ_l. As is shown in detail in Ref. 13, the resulting series behaves, to leading order, as $S_{ij/kl}/(1-p)$, independent of the values of p_c and the critical exponents. Thus,

$$S_{ij/kl}=\lim_{n\to\infty} c_n^{ij/kl} ,$$

and estimates for $S_{ij/kl}$ are obtained by extrapolation of the series coefficients. The resulting estimates are displayed in Table VI. The errors quotes are those of the extrapolation procedure. We list the new estimates obtained for $S_{24/33}$ and $S_{25/34}$, and compare them with the ϵ-expansion values and the values obtained by Adler *et al.*[5] translated into our terms. Note that our estimates are for amplitude ratios on the same side of the transition. Amplitude ratios from both sides of the transition are harder to estimate, and this may be the cause of the discrepancy between continuum and lattice percolation values. We have learned[51] that our results have stimulated some work on the determination of this kind of ratios for the continuum percolation problem.

V. CONCLUSIONS AND COMPARISONS WITH OTHER RESULTS

Our new exponent and threshold values have been entered in Tables I and II. Overall we see a very pleasing improvement in accuracy of evaluation. The increase in accuracy with respect to our calculations from the shorter series is at least tenfold for most exponents. We must emphasize that our error estimates often tend to be substantially larger than those of series calculations based on d log Padé analysis, since we quote a final range based on all possible convergences in the h,Δ_1 planes of the threshold range where some convergence is seen. Thus, it is very unlikely that the true result is outside our error bars. In usual d log Padé analysis values for $\Delta_1=1.0$ only are included. The increase in accuracy is largest for β, since the higher moments used in the β determination converged much better than did the 11th-order ones.

An increase in the extent of agreement with results from the ϵ expansion can also be seen. For $d=4$ and 5 our results for γ and β agree completely to the accuracy of both calculations, and our results now have less spread than that between some of the different extrapolations from the third-order ϵ expansions. In five dimensions the γ estimate has moved much closer to the ϵ-expansion result, without a large shift in central threshold estimate. In four dimensions, despite a relatively large movement in optimal threshold, the value has remained close. The β estimates are extremely close in both dimensions. The values for ν, which are obtained from our series results

TABLE VI. Amplitude ratios.

Dimension	6	5	4	3	2	1
$S_{24/33}$						
Exact, Ref. 5	$\frac{1}{2}$					$\frac{2}{3}$
Series, this work		0.490±0.002	0.475±0.005	0.436±0.005	0.37±0.01	
$\frac{1}{2}(1-0.011\,95\epsilon-0.011\,322\epsilon^2)$		0.488	0.465	0.431	0.386	
$\frac{1}{2}/(1+0.011\,95\epsilon+0.011\,469\epsilon^2)$		0.488	0.467	0.439	0.406	
Series, Ref. 5		0.50	0.48	0.43	0.35	
$S_{25/34}$						
Exact, Ref. 5	$\frac{1}{3}$					$\frac{5}{9}$
Series, this work		0.31±0.1	0.29±0.1	0.25±0.2	0.15±0.5	
$\frac{1}{3}(1-0.019\epsilon-0.0149\epsilon^2)$		0.322	0.301	0.270	0.229	
$\frac{1}{3}/(1+0.019\epsilon+0.0153\epsilon^2)$		0.322	0.303	0.279	0.252	
Series, Ref. 5		0.33	0.30	0.26	0.18	

via hyperscaling, are in excellent agreement with the ϵ expansion in all dimensions. This lends credence to the common belief that hyperscaling holds for percolation in $2 \leq d \leq 6$. Our new threshold estimate in four dimensions is much closer to that found by Grassberger[26] than our older estimate was. We do not have any comparison for the five-dimensional threshold that is of comparable accuracy and reliability.

At the conclusion of our original analysis, three dimensions remained the only possible source of unhappiness. In our past calculations for three-dimensional percolation there has been a tendency to use Monte Carlo threshold values.[12,22] With the extension of the moment series to 15 terms an independent threshold determination seemed to be possible and was carried out. During the early stages of this analysis we were rather concerned that the thresholds at which convergence was seen failed to overlap with some of the Monte Carlo estimates. We were relieved to receive information[36,37] that more recent Monte Carlo results indeed were close to the threshold values that we were calculating. As can be seen in Table II, the new results for the bond simple-cubic threshold are in excellent agreement with our value, and somewhat below the old simulation values. For the body-centered-cubic problem our threshold is above the old series value, and we are not aware of any other recent calculations for this system.

Unfortunately, as we write this there is not as complete a consensus on exponent values. While there is excellent agreement between our calculations and those of Ref. 37, there remains a discrepancy with the field theoretic values. The field theories give similar β estimates that are only some 80% of the older series and Monte Carlo estimates. It is not clear how reliable ϵ-expansion results should be at three dimensions, but the direct-loop vertex calculations should be useful.[16] Our results fall about midway between the older series and the older Monte Carlo results. Thus, our results and those of Ref. 37 are still a little different from the field theoretic exponents. It must be noted that we have two quite independent ways to obtain β. Since one of these is from the high-density series via direct measurement of β and the second from the low density via evaluation of Δ, the chances of there being systematic errors in the measurements are greatly reduced. The high-density series estimates are a little higher than the low-density ones, although the error regions overlap. For γ percentagewise discrepancies are much smaller. Our results are probably more reliable than the older series results, since they are based on longer series. The fact that both our results and those of Ref. 37 fall midway between the old Monte Carlo and the field theories for β would seem to suggest that they are the most likely to be correct. (It should be noted that while our central estimates are in excellent agreement with those of Ref. 37 we claim a lower precision for reasons of possible systematic corrections caused by higher-order correction terms. We rather think such corrections should also be present in the simulations.) However, whatever the error range, it is now clear that η is negative for three-dimensional percolation.

Our series amplitude ratios are in good agreement with the ϵ-expansion results; in the lower dimensions the improvement over the results of Ref. 5 is most pleasing. This improvement further strengthens the claims made in Ref. 5 concerning the reliability of the ϵ expansion down to $d=2$. At present we still cannot make a comparison with simulation values and we hope that this will become possible in the future.

The final results to discuss are those for the correction to scaling exponent Δ_1. In addition to the estimates given in Table I, we can compare our values with results obtained[52] for Ω, the correction to scaling exponent in the field direction. It has been proposed[1] that $\Omega\beta\delta=\Delta_1$, or $\Omega\Delta=\Delta_1$ from scaling arguments, and despite apparent problems with this relation in 2D isotropic percolation,[53,54] it has been shown[55] to be reliable for directed percolation in higher dimensions. This relation gives central Δ_1 estimates of 0.33–1.01, 0.41, and 0.88 for five, four, and three dimensions, respectively, using the Δ values of our calculations. Comparison of these estimates with those quoted in Table I, suggests that in five dimensions the comparison is inconclusive because of the large range of the Ω estimate. In four dimensions it appears that we are not observing Ω and Δ_1 values that correspond via these scaling relations. In three dimensions it is possible that the measured Δ_1 and Ω estimates do satisfy the scaling relation. Further effort towards checking these relations via better calculations of Ω would be most desirable.

We may observe from Table I that there is far less agreement between the different correction exponent values than is the case for dominant exponents, thresholds or amplitude ratios. Nevertheless, in five dimensions, our Δ_1 estimate includes both the scaling field[19] and ϵ-expansion values[33] within its error ranges. Since our measurement falls between the other two it would seem very likely that it is a reliable choice. There is something of a discrepancy between some of the calculations in four dimensions, but the fact that the evaluation of correction exponents is a higher-order problem, would lead one to expect less precision than for dominant exponents. This could be an adequate explanation for these discrepancies, were it not for the overall dimension trends. Our value is close to that of Grassberger,[26] and both are a little below the field theoretic estimates. In three dimensions, however, the discrepancy between our value and that of the ϵ-expansion is such that we can in no way claim to be measuring the same exponent. Grassberger's value is even lower than both. The ϵ-expansion correction comes from the most nearly relevant correction term in 6-ϵ dimensions. There is no *a priori* reason to expect that this correction will remain the most relevant down to three dimensions. The fact that the scaling field estimate in three dimensions is also below the ϵ-expansion result lends credence to the possibility than an operator that was more irrelevant near six dimensions has crossed over somewhere near four dimensions, and gives the most relevant correction in three dimensions. This is because in the scaling field picture (see Fig. 5 of Ref. 19) there is exactly such a crossover just above four dimensions and the second most relevant correction has a value that is about the same as the ϵ-

expansion value. Furthermore, in Ref. 22 a second correction was seen in one of the 3D series calculations at approximately this location ($\Delta_1 \approx 1.8$). This crossover scenario is also consistent with the slightly higher values that both the scaling field and ϵ-expansion methods obtain in four dimensions, since the approximation to the actual dimensional location of the crossover could vary slightly between the series and field theoretic results. Our overall conclusion is that there is apparently a crossover of irrelevant operators between three and six dimensions and further elucidation of its nature could prove interesting. We may add that while the series in four and five dimensions clearly exhibit nonanalytic corrections to scaling it is possible that the 3D value of $\Delta_1 = 1.1 \pm 0.2$ is an analytic correction. The situation is somewhat reminiscent of 2D directed percolation,[56] where it is also unclear whether the measured correction is actually an analytic term of not. In the directed percolation case $M2$ gave resonances, suggesting a simple analytic form.[56] Here this is not the case. In both cases comparison with field theoretic values suggests that there could be a close to, but not exactly, analytic correction and unequivocal determination is probably extremely difficult.

In conclusion, we have succeeded in proposing a consistent set of dominant critical exponents, amplitude ratios and thresholds for isotropic percolation above two dimensions. We have also summarized existing information for isotropic percolation, noting that where different calculations have been made, agreement is excellent for all but the correction exponents. It is to be hoped that further work will be done via simulation on percolation amplitude ratios. We have proposed a scenario for some of the discrepancies in the correction behavior and hope that further calculations will be undertaken in order to test this hypothesis.

The most important implications of our work are twofold, and extend beyond the isotropic percolation problem. Firstly, the complete agreement with the alternately derived 3D series of Ref. 23 (which is one term shorter) shows that both algorithms for series development must be correct. This is an extremely powerful check on our NFE method, and on the computer programs that have been and will be used for many different problems. Secondly, the comparison with the newest[36,37] 3D simulations shows beyond all doubt that a series of sufficient length, properly analyzed, yields results which are competitive with the best alternative calculations. Since the series require considerably less computer time than most alternative methods, and our algorithm enables simultaneous determination of series for all dimensions, this is most pleasing.

ACKNOWLEDGMENTS

This work was supported in part by grants from the Israel Academy of Sciences and Humanities, and by the U.S.-Israel Binational Scienc Foundation. Also A.B.H. acknowledges partial support from the Materials Research Laboratory (MRL) program of the National Science Foundation under Grant No. DMR 85-19059. We thank D. Stauffer and R. Ziff for informing us about their unpublished results, and E. Riedel and K. Newman for providing us with the raw data from which their figures were constructed. One of us (J.A.) acknowledges support from the Technion Vice President Research Fund and from the New York Metropolitan Fund.

APPENDIX A: MEAN-FIELD FREE ENERGY AS A FUNCTION OF FIELD INCLUDING CORRECTIONS TO SCALING

The simplest way to obtain the corrections to the dominant singular terms in the free energy is to calculate these corrections to the moments of the cluster-size distribution for the Cayley tree. Results for the Cayley tree of coordination number z should asymptotically agree with those of the hypercubic lattice in d dimensions for $z = 2d$ in the limit $d \to \infty$. To start with, we note that the zero-field free energy has no corrections to the first two terms in Eq. (2.18). This can be seen by using Eq. (2.16) inasmuch as $B = 0$ when $h = 0$. Also $\partial F / \partial h = 0$ for $p < p_c$. Thus, we may limit our consideration to corrections to $\Gamma_q(p)$ for $q \geq 2$. These are most easily found using the recursion relation[57] for $q \geq 2$,

$$\Gamma_{q+1} = [p(1-p)\partial \Gamma_q / \partial p + (1+p)\Gamma_q]/(1-\sigma p) . \tag{A1}$$

For $\sigma > 1$ we set

$$\Gamma_{q+2} = A_q (p_c - p)^{(-2q-1)} + B_q (p_c - p)^{-2q} \tag{A2}$$

with $A_0 = (\sigma+1)/\sigma^2$ and $B_0 = -1/\sigma$, i.e.,[7]

$$\Gamma_2 \equiv \chi^0 = (1+p)/(1-\sigma p) .$$

Then (A1) yields

$$A_q = \left[\frac{\sigma - 1}{\sigma^3} \right] (2q-1) A_{q-1} , \tag{A3a}$$

$$B_q = \left[\frac{\sigma - 1}{\sigma^3} \right] (2q-2) B_{q-1} + A_{q-1} \left[\frac{\sigma+1}{\sigma^2} - \frac{\sigma-2}{\sigma^2}(2q-1) \right] . \tag{A3b}$$

Solving (A3) we obtain

$$A_q = \frac{(q - \frac{1}{2})!}{(-\frac{1}{2})!} \frac{\sigma+1}{\sigma^2} \left[\frac{2(\sigma-1)}{\sigma^3} \right]^q , \tag{A4a}$$

$$\beta_q \equiv \frac{B_q}{A_q} = \frac{\sigma}{\sigma - 1} \left[\frac{(4-2\sigma)q + 2\sigma + 5}{3} \right], \quad q \geq 2 , \tag{A4b}$$

and $\beta_0 = -\sigma/(\sigma+1)$. Thus,

$$\Gamma_{q+2} = \frac{A_q}{(p_c - p)^{2q+1}} [1 + \beta_q (p_c - p)] . \tag{A5}$$

Having determined the corrections to all the derivatives of F with respect to h, we can construct the corrections to F itself, the result being given in (2.18).

APPENDIX B: SITE-BOND GENERATING FUNCTION

To get the site-bond distribution function[43,44] one considers the Potts model with anisotropic interactions

$$H=-K_1\sum_{\langle x,x'\rangle}\delta_{s(x),s(x')-1}-K_2\sum_{\langle x,x'\rangle}\delta_{s(x),s(x')-1}\delta_{s(x),1}\,,$$
$$-h\sum_x(q\delta_{s(x),1}-1) \tag{B1}$$

where

$$K_2=-\ln[1-p+p\exp(-K)]$$

and

$$K_1=\ln\{1+[p\exp(-K)]/(1-p)\}\,.$$

Now the free energy is the following generalization of (2.2):

$$F=h+\sum_{n_s;n_b}W(n_s,n_b,p)\exp(-n_sh-n_bK)\,, \tag{B2}$$

where $W(n_s,n_b,p)$ is the average number of clusters per site having n_s sites and n_b bonds at bond concentration p. When K is nonzero, K_2 is nonzero and the development in the text must be revised as follows: Equation (2.11) becomes

$$\exp[-B]=1-p+p\exp[-(h+K+\sigma B)]\,, \tag{B3}$$

and (2.13) remains valid but Eq. (2.24b) becomes

$$Y(\Gamma)=[n_b(\Gamma)-n_s(\Gamma)]\exp[-(h+zB)]$$
$$-(1-p)n_b(\Gamma)\exp[-(h+\sigma B)]$$
$$+\sum_{C\in\Gamma}P(C;\Gamma)\exp\left[-\sum_{x\in C}\tilde{h}(x)-Kn_b(C)\right]\,, \tag{B4}$$

where $n_b(C)$ is the number of bonds in the cluster C.

[1] J. W. Essam, in *Phase Transitions and Critical Phenomena,* edited by C. Domb and M. S. Green (Academic, New York, 1972), Vol. 2; Rep. Prog. Phys. **43**, 833 (1980); *Annals of the Israel Physical Society,* edited by G. Deutscher, R. Zallen, and J. Adler (Hilger, London, 1983), Vol. 3.

[2] A. Aharony, in *Directions in Condensed Matter Physics,* edited by G. Grinstein and G. Mazenko (World-Scientific, Singapore, 1986), p. 1; D. Stauffer, Phys. Rep. **54**, 1 (1979); *Introduction to Percolation Theory* (Taylor and Francis, London, 1985).

[3] J. W. Essam, D. S. Gaunt, and A. J. Guttmann, J. Phys. A **11**, 1983 (1978).

[4] A. Aharony, Phys. Rev. B **22**, 400 (1980).

[5] J. Adler, A. Aharony, Y. Meir, and A. B. Harris, J. Phys. A **19**, 3631 (1986).

[6] B. Nienhuis, J. Phys. A **15**, 199 (1982); M. P. M. den Nijs, *ibid.* **12**, 1857 (1979); B. Nienhuis, E. K. Riedel, and M. Schick, *ibid.* **13**, 189 (1980); R. B. Pearson, Phys. Rev. B **22**, 2579 (1980).

[7] M. E. Fisher and J. W. Essam, J. Math. Phys. **2**, 609 (1961).

[8] H. Kesten, *Percolation for Mathematicians* (Birkhauser, Boston, 1982).

[9] D. Stauffer, Phys. Lett. **83A**, 404 (1981).

[10] F. Fucito and E. Marinari, J. Phys. A **14**, L85 (1981); F. Fucito and G. Parisi, *ibid.* **14**, 507 (1981).

[11] J. Adler, M. Moshe, and V. Privman, Phys. Rev. B **26**, 1411 (1982).

[12] J. Adler, M. Moshe, and V. Privman, in *Annals of the Israel Physical Society,* edited by G. Deutscher, R. Zallen, and J. Adler (Hilger, London, 1983), Vol. 3. This paper contains a discussion on convergence criteria for $M2$.

[13] Y. Meir, J. Phys. A **20**, L349 (1987).

[14] A. B. Harris, T. C. Lubensky, W. K. Holcomb, and C. Dasgupta, Phys. Rev. Lett. **35**, 327 (1975); **35**, 1397E (1975).

[15] J. Adler, Phys. Rev. Lett. **57**, 916 (1986).

[16] J. S. Reeve, J. Phys. A **15**, L521 (1982); J. S. Reeve, A. J. Guttmann, and B. Keck, Phys. Rev. B **26**, 3923 (1982).

[17] D. Y. Kim, H. J. Heermann, and D. P. Landau, Phys. Rev. B **35**, 3661 (1987); I. Balberg, *ibid.* **37**, 2391 (1988).

[18] A. Margolina, H. J. Herrmann, and D. Stauffer, Phys. Lett. **93A**, 73 (1982); D. W. Heermann and D. Stauffer, Z. Phys. B **44**, 339 (1981).

[19] K. Newman, E. K. Riedel, and S. Muto, J. Phys. B **29**, 302 (1984).

[20] D. S. Gaunt, S. G. Whittington, and M. F. Sykes, J. Phys. A **14**, L247 (1981).

[21] D. S. Gaunt and M. F. Sykes, J. Phys. A **16**, 783 (1983).

[22] J. Adler, Z. Phys. B **55**, 227 (1984).

[23] M. F. Sykes and M. K. Wilkinson, J. Phys. A **19**, 3415 (1986).

[24] D. Stauffer and J. G. Zabolitzky, J. Phys. A **19**, 3705 (1987); S. Wilke, Phys. Lett. **96A** 344, (1983).

[25] P. Grassberger, J. Phys. A **19**, L241 (1986).

[26] P. Grassberger, J. Phys. A **19**, 1681 (1986).

[27] R. Fisch and A. B. Harris, Phys. Rev. B **18**, 416 (1978).

[28] D. S. Gaunt and H. Ruskin, J. Phys. A **11**, 1369 (1978).

[29] H. Saleur and B. Derrida, J. Phys. (Paris) **46**, 1043 (1985).

[30] O. F. de Alcantara Bonfim, J. E. Kirkham, and A. J. McKane, J. Phys. A **13**, L247 (1980); **14**, 2391 (1981).

[31] S. Kirkpatrick, Phys. Rev. Lett. **36**, 69 (1976).

[32] N. Jan, D. C. Hong, and H. E. Stanley, J. Phys. A **18**, L935 (1985).

[33] J. Adler, A. Aharony, and A. B. Harris, Phys. Rev. B **30**, 2832 (1984).

[34] J. Adler, A. Aharony, Y. Meir, and A. B. Harris, Phys. Rev. B **34**, 3469 (1986).

[35] In general, the accuracy to which critical exponents have been measured for three-dimensional percolation has lagged behind that obtained for the $d=3$ Ising model. We must place less confidence on ϵ-expansion results for pecolation at $d=3$ since $\epsilon=3$ rather than $\epsilon=1$, as in the Ising model. There is, however, no obvious *a priori* reason in the physics of the problems for the considerably less precise measurements of thresholds for percolation relative to the Ising model. For the Ising model on the sc lattice $T_c=0.221\,656\pm0.000\,005$ from Monte Carlo renormalization-group calculations [G. S. Pawley, R. H. Swendsen, D. J. Wallace, and K. G. Wilson, Phys. Rev. B **29**, 4030 (1983)] in excellent agreement with the series value $T_c=0.221\,655\pm0.000\,005$ [J. Adler, J. Phys. A **16**, 3585 (1983)], obtained by the analysis methods that are used in this paper.

[36]D. Stauffer, H. E. Stanley, and H. J. Herrmann (private communication).
[37]R. M. Ziff and G. Stell (private communication).
[38]L. Klein, J. Adler, A. Aharony, A. B. Harris, and Y. Meir, Bull. Israel Phys. Soc. **35**, 11 (1989); Phys. Rev. B **40**, 4824 (1989).
[39]A. B. Harris, Phys. Rev. B **26**, 337 (1982).
[40]A. B. Harris and Y. Meir, Phys. Rev. A **36**, 1840 (1987).
[41]P. W. Kasteleyn and C. M. Fortuin, J. Phys. Soc. Jpn. Suppl. **26**, 11 (1969); C. M. Fortuin and P. W. Kasteleyn, Physica (Utrecht) **57**, 536 (1972).
[42]A. B. Harris, J. Phys. A **20**, L1011 (1987); **20**, 5405 (1987).
[43]M. J. Stephen, Phys. Rev. B **15**, 5674 (1977); M. Giri, M. J. Stephen, and G. S. Grest, *ibid.* **16**, 4971 (1977).
[44]A. B. Harris and T. C. Lubensky, Phys. Rev. B **23**, 3591 (1981); **24**, 2656 (1981).
[45]J. Adler, M. Moshe, and V. Privman, Phys. Rev. B **26**, 3958 (1982).
[46]J. Adler, J. Phys. A **18**, 307 (1985); Phys. Rev. B **31**, 4693 (1985).
[47]V. Privman, J. Phys. A **16**, 3097 (1983).
[48]J. Adler, M. Moshe, and V. Privman, J. Phys. A **14**, L363 (1981); see also, J. Adler and I. G. Enting, *ibid.* **17**, 2233 (1984).
[49]J. Adler and V. Privman, J. Phys. A **14**, L463 (1981). This reference includes a discussion of test series work for this method.
[50]D. L. Hunter and G. A. Baker, Jr., Phys. Rev. B **7**, 3346 (1973).
[51]J. Balberg (private communication).
[52]H. Nakanishi and H. E. Stanley, Phys. Rev. B **22**, 2466 (1980).
[53]J. Adler, Phys. Rev. B **31**, 4693 (1985).
[54]A. Aharony and M. E. Fisher, Phys. Rev. B **27**, 4394 (1983).
[55]J. Adler and J. A. M. S. Duarte, Phys. Rev. B **35**, 7046 (1987); J. Adler, J. Berger, J. A. M. S. Duarte, and Y. Meir, *ibid.* **37**, 7529 (1988).
[56]J. W. Essam, K. De'Bell, J. Adler, and F. M. Bhatti, Phys. Rev. B **33**, 1982 (1986).